MAGNETOTRANSPORT STUDIES OF DIVERSE ELECTRON SOLIDS IN A

TWO-DIMENSIONAL ELECTRON GAS

A Thesis

Submitted to the Faculty

of

Purdue University

by

Vidhi Shingla

In Partial Fulfillment of the

Requirements for the Degree

of

Doctor of Philosophy

August 2019

Purdue University

West Lafayette, Indiana

THE PURDUE UNIVERSITY GRADUATE SCHOOL
STATEMENT OF THESIS APPROVAL

Dr. Gábor A. Csáthy, Chair

    Department of Physics and Astronomy

Dr. Leonid Rokhinson

    Department of Physics and Astronomy

Dr. Rudra R. Biswas

    Department of Physics and Astronomy

Dr. Chen-Lung Hung

    Department of Physics and Astronomy

Approved by:

    Dr. John P. Finley

        Head of the Graduate Program

Dedicated to my father

ACKNOWLEDGMENTS

The journey towards getting this degree has been a long one and it would not be possible without the support from many people. The most significant part was played by my advisor Prof. Gábor Csáthy who invested in me to become a better physicist. He spent countless hours training me with the intricacies of cryogenics and sophisticated electronic techniques. I am truly grateful to him for his exceptional motivation and encouragement through the many failures before getting it right. Gábor was always deeply devoted to my success with a lot of advice and suggestions for succeeding ahead of this degree. I thank him for being a remarkable mentor in every way.

I would like to thank my committee members, Dr. Leonid Rokhinson, Dr. Chen-Lung Hung and Dr. Rudro Biswas for investing the time in learning about my project and helping me achieve my goals. I would like to acknowledge Dr. Loren Pfeiffer and Dr. Ken West at Princeton University for the high quality of samples provided which were instrumental for my project.

I am grateful to my past senior labmate Ethan Kleinbaum for introducing me to cryogenics and cleanroom fabrication. He served as a great mentor in my initial year in the lab and continues to play that role. I am thankful to Katherine Schreiber for always patiently lending an ear to the progress of my project and answering a lot of my questions. I thank my junior labmate Kevin and other graduate students in the department including Ananthesh, Tailung, Zhujing, Ali, Antoine and Jimmy for lending a hand in the lab at odd hours.

Many staff members in the Department of Physics contributed in many ways to make this degree possible with their support. Sandy Formica served as the to-go person for almost everything and always found a way around administrative road-blocks. I thank Keith Schmitter who works tirelessly for keeping a continuous supply

of helium running which was central to all my experiments, Mark Smith for providing support with electronics, Jim Corwin for his assistance and help in the machine shop and Jessica Holsinger from Science IT for rescuing me from the many issues with lab computer networks.

The many years spent towards completing this degree were made memorable because of many friends. I especially thank Mary Ann and Dave for making me feel at home in the US. Antoine, Yifei, Ananthesh, Swati and Lois were part of many light-hearted times spent which helped balance the long hours working in the lab. A special thanks to Lavish for always patiently listening to many detailed tales of my graduate life and for all the encouragement.

The love and support from my family was unmatched during these years. Words are not enough to express my gratitude for my brother-in-law Reto and both my sisters Syona and Richa. They constantly looked out for me and shared the excitements of my project with joy. This degree would not be possible without the constant pillar of support that my mother provided during some of the very tough times. She made many sacrifices to help me get this far. I thank her for her strength, patience and for making me who I am. I deeply wish that my father was able to see me complete this degree for which he greatly encouraged me. I apologize to him for taking longer than he could wait and to him I dedicate this thesis.

TABLE OF CONTENTS

LIST OF FIGURES

ABSTRACT

Shingla, Vidhi Ph.D. Candidate, Purdue University, August 2019. Magnetotransport Studies of Diverse Electron Solids in a Two-Dimensional Electron Gas. Major Professor: Gábor A. Csáthy.

The two dimensional electron gas subjected to a perpendicular magnetic field is a model system that supports a variety of electronic phases. Perhaps the most well-known are the fractional quantum Hall states, but in recent years there has been an upsurge of interest in the charge ordered phases commonly referred to as electron solids. These solids are a consequence of electron-electron interactions in a magnetic field. While some solid phases form in the lowest Landau level, the charged ordered phases are most abundant in the higher Landau levels. Examples of such phases include the Wigner solids, electronic bubble phases and stripe or nematic phases. Open questions surround the exact role of disorder, confinement potential, temperature and the Landau level index in determining the stability and competition of these phases with other ground states.

The interface of GaAs/AlGaAs remains the cleanest host for the two-dimensional electron gas due to the extremely high quality of materials available and the advancement in molecular beam epitaxy growth techniques. As a result, exceptionally high electron mobilities in this system have been instrumental in the discovery of numerous electron solids.

In this Thesis, I discuss the discovery and properties of several electron solids that develop in such state-of-the-art two dimensional electron gases. These electron solids often develop at ultra low temperatures, in the milliKelvin temperature range. After an introduction to the physics of the quantum Hall effect in two dimensions, in chapter 3, I discuss electron solids developing in the $N=1$ Landau level. While these solids have been known for some time, details of the competition of these phases

with the nearby fractional quantum Hall states remains elusive. A number of reports observe new fractional quantum Hall states at filling factors where electron solids are found in other experiments. We undertook a systematic study to answer some of these unsettled questions. We see evidence for incipient fractional quantum Hall states at 2+2/7 and 2+5/7 at intermediate temperatures which are overtaken by the electronic bubble phases at lower temperatures. Several missing fractional states including those at filling factors 2+3/5, 2+3/7, 2+4/9 highlight the relative stability of the electronic solids called the bubble phases in the vicinity in our sample.

In chapter 4, I discuss a newly seen electron crystal which manifests itself in transport measurements as a reentrant integer quantum Hall state. Reentrant integer behavior is common in high Landau levels, but so far it was not observed in the lowest Landau level in narrow quantum well samples. In contrast to high Landau levels, where such reentrant integer behavior was associated with electronic bubbles, we believe that the same signature in the N=0 Landau level is due to an electronic Wigner crystal. The filling factors at which we observe such reentrance reveal that it is a crystal of holes, rather than electrons. The discovery of this reentrant integer state paints a complex picture of the interplay of the Wigner crystal and fractional quantum Hall states.

Finally, in chapter 5, I discuss the observation of a novel phenomenon, that of reentrant fractional quantum Hall effect. In the lowest Landau level, we observe a fractional quantum Hall state, but as the field is increased, we see a deviation and then a return to quantization in the Hall resistance. Such a behavior indicates a novel electron solid. In contrast to the collective localization of electrons evidenced by the reentrant integer quantum Hall effect, such reentrance to a fractional Hall resistance clearly points to the involvement of composite fermion quasiparticles. This property thus distinguishes the ground state we observed as a solid formed of composite fermions. Such a solid phase is evidence for exotic electron-electron correlations at play which are clearly different from those in the traditional Wigner solid of electrons.

1. THE QUANTUM HALL EFFECT

Electrons confined to two-dimensions at the interface of semiconductor heterostructures has important technological applications in electronic components such as transistors, light emitting diodes (LEDs) and Hall sensors as few examples. The same system when cooled to low temperatures in the presence of a perpendicular magnetic field exhibit a variety of quantum-mechanical ground states. In this chapter, I will introduce the physics of the two-dimensional electron gas in strong magnetic fields including the quantum Hall effect resulting from confined dimensionality and discuss the physics of the two-dimensional electron gas in GaAs/AlGaAs as the host material.

1.1 Integer Quantum Hall Effect

The Integer Quantum Hall Effect was discovered in 1980 by Klaus von Klitzing in a Si-MOSFET (metal oxide-semiconductor field-effect transistor) at 1.5K subjected to magnetic field of the order of 20T [1]. The basic Hall measurement setup is shown in Figure 1.1. A 4-wire measurement of voltage transverse to the excitation current yields the Hall resistance R_{xy} and likewise the magnetoresistance R_{xx}. The classical picture predicts a linear dependence of Hall resistance on the magnetic field. However, Klitzing's experimental results as shown in Figure 1.2 show a plateau in Hall resistance at h/ie^2 where i is an integer with the longitudinal resistance R_{xx} vanishing at those corresponding electron densities controlled by the gate voltage. This discovery marks the *first* observation of topological phases of matter in contrast to the conventional Landau phases which are understood in terms of different symmetries of the Hamiltonian. These integer quantum Hall states possess the *same* symmetry of the Hamiltonian. The different phases arise due to the existence of a discrete energy gap unaffected by continuous small variations of the potential term in the Hamiltonian.

These phases are therefore independent of local perturbations and are topologically robust.
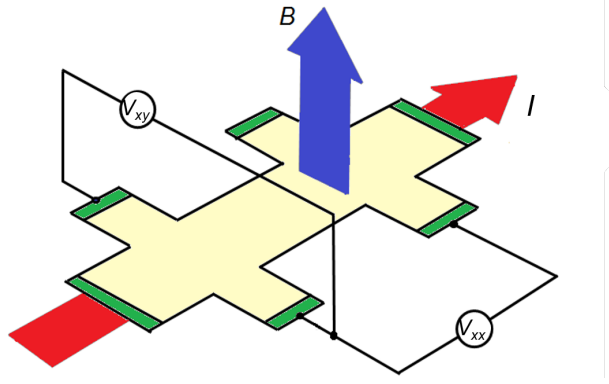
Figure 1.1. The basic measurement setup to determine the transport coefficients. A magnetic field B is applied perpendicular to the applied current I. The voltage measured along the direction of current then yields the longitudinal resistance $R_{xx} = V_{xx}/I$ and voltage measured in the transverse direction gives the Hall resistance $R_{xy} = V_{xy}/I$.

The formation of the discrete energy levels is derived by solving the Schrödinger equation of a single electron confined in two dimensions in a magnetic field. The Hamiltonian of a spinless electron in a uniform magnetic field B characterized by a vector potential $\vec{A}$, given by [17]

$$H = \frac{\left(\vec{p} - e\vec{A}\right)^2}{2m} \tag{1.1}$$

The above Hamiltonian is solved for the case of a perpendicular magnetic field in the z-direction given by $\vec{B} = B\hat{z}$. The vector potential is chosen to be the Landau gauge given by $\vec{A} = Bx\hat{y}$. Solving this equation for the eigenvalues yields the familiar simple harmonic oscillator energy values given,

$$E_n = \hbar\omega_c(n + \frac{1}{2}) \tag{1.2}$$

where n is an integer and $\omega_c = eB/m$. The mass m is the mass of an electron which in a condensed matter environment refers to the band mass. Each of these energy
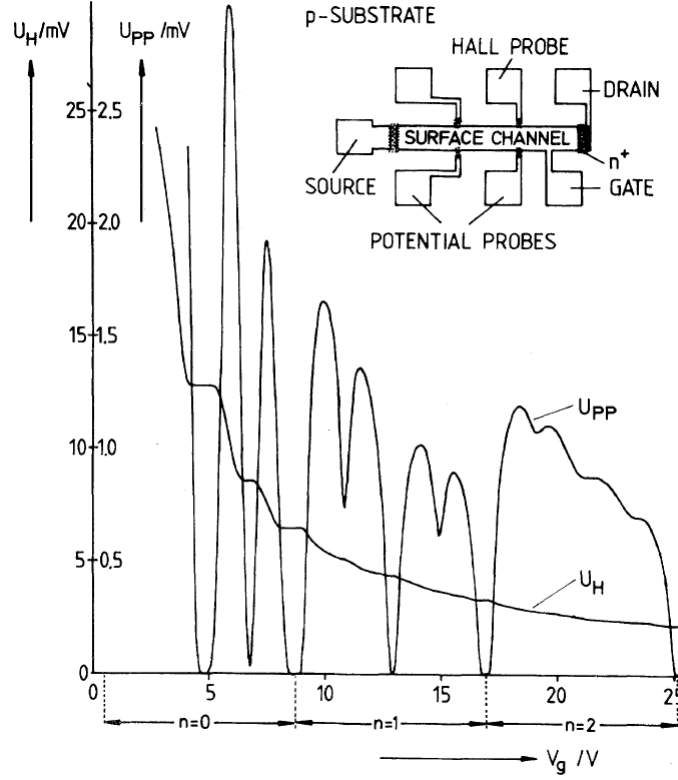
Figure 1.2. The original plot for the first discovery of the Integer Quantum Hall Effect. Hall Voltage U_H and longitudinal voltage U_{pp} is plotted as function of gate voltage V_g at temperature $T = 1.5K$. Inset show the sample sketch in a Hall bar geometry. Reprinted figure with permission from K. von Klitzing et al., Phys. Rev. Lett. 45, 494 (1980). Copyright 1980 by the American Physical Society.

levels is called a Landau Level with $\hbar\omega_c$, the cyclotron gap between each of these levels. These Landau levels are degenerate with degeneracy given by $D = eB/h$. The number of filled Landau levels is referred to as the *filling factor* denoted by ν and is given by

$$\nu = n_s/D = n_s h/eB \tag{1.3}$$

where n_s is the 2DEG electron density. If in addition, the electron spin is included, the Zeeman term appears in the Hamiltonian due to the coupling of the electron spin to the external magnetic field B. This coupling is given by

$$H_Z = -\vec{\mu} \cdot \vec{B} \tag{1.4}$$

where $\vec{\mu}$ is the magnetic dipole moment of the electron given by $\vec{\mu} = \frac{g\mu_B \vec{S}}{\hbar}$. The eigenvalues of this Hamiltonian for $\vec{B} = B\hat{z}$ is $E_Z = \pm\frac{1}{2}g\mu_B B$. In Figure 1.3, a pictorial representation of the discrete Landau levels is shown. In addition to the
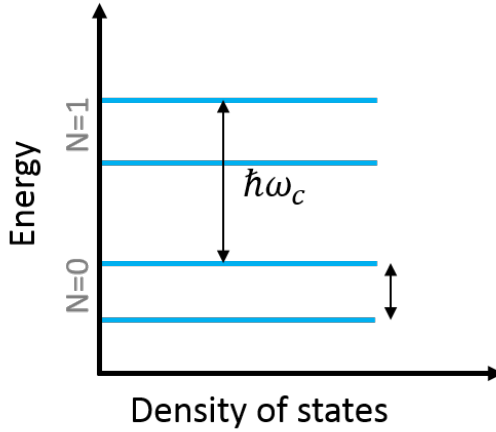
Figure 1.3. The discrete Landau levels with each level spin split due to the Zeeman coupling.

spin degree of freedom, a valley degeneracy can further split the Landau levels which is absent for the case of GaAs. Energy level shifts due to spin-orbit coupling play a minor role in this system.

The quantization in Hall resistance can then be understood in terms of these filling Landau levels with the filling factor denoted by ν. The confinement to two-dimensions is essential for this discrete set of energy levels effect as the motion along the magnetic field can add any amount of energy to the Landau levels and as a result, there are no quantized levels in three dimensions.

The Landau levels shown in Figure 1.3 denote the energy levels in the ideal limit with no defects and impurities in the sample. However, realistic samples have a finite disorder which broadens these levels in two ways. The defects in the sample cause Anderson localization [2] which is schematically depicted in Figure 1.4 (a) as the localized states in light blue. The other effect is broadening the center of the single particle energy levels into extended states which exist throughout the sample.
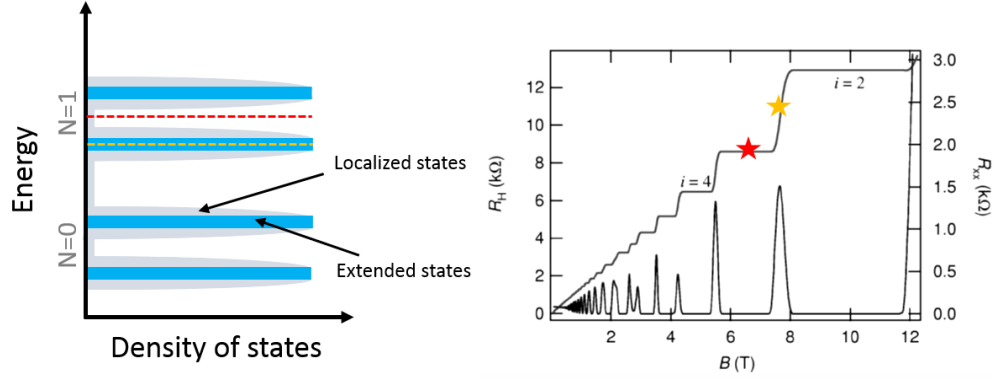
Figure 1.4. (a) A sketch showing extended and localized states as a result of disorder. Fermi energy at two different points while changing the magnetic field. (b) Integer Quantum Effect in AlGaAs/GaAs with quantum states marked by integers. Figure adapted from ref. [11].

This broadening of the Landau levels is the very reason for the long stretches of quantized Hall values. When the Fermi level (E_F) moves through the extended states, normal electron conduction takes place and we see R_{xx} increasing with B field as indicated by the yellow star in Figure 1.4 (b). On reducing the magnetic field and thereby changing the degeneracy of each level, E_F moves through the localized states which do not conduct leading to the wide plateaus in R_{xy}.

However, the natural question arises on why R_{xx} vanishes while the localized states do not conduct. This brings the edge states into picture which are a hallmark of topological phases, in general. As seen in the Figure 1.5a, the Fermi energy intersects the confining potential due to the finite geometry of the sample which causes these

edge modes to exist. From a semi-classical point of view, with a filled Landau level, the cyclotron motion of the electrons causes the *bulk* to be insulating while at the edges, skipping orbits form.
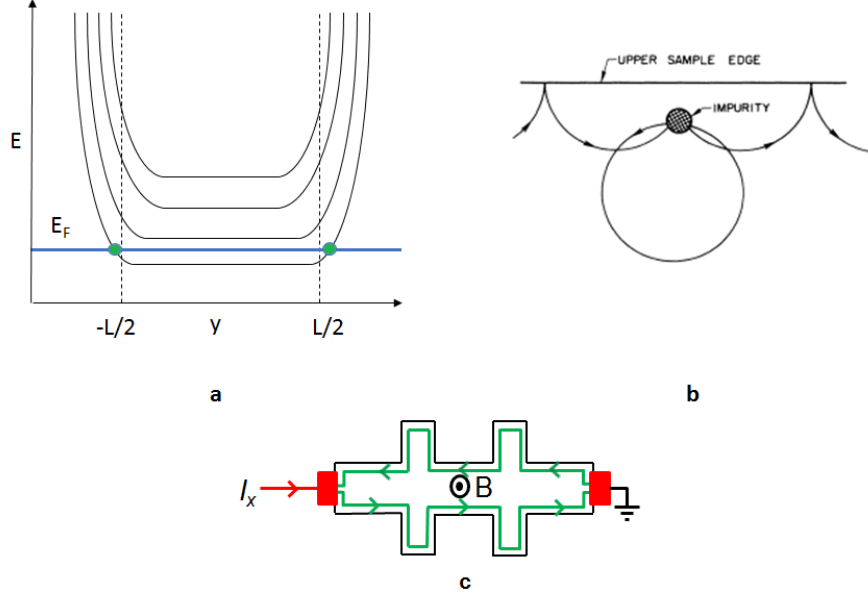
Figure 1.5. **a**) Edge states in a sample of length L showing the bending of Landau levels due to the confinement potential of the sample geometry. The Fermi level intersects these Landau level resulting in conducting states at the edges. Adapted from [12].**b**) Semi-classical picture showing skipping cyclotron orbit at the edge of the sample. Due to suppressed backscattering, these edge modes are dissipationless. [12]. Reprinted figure with permission from Büttiker et al., Phys. Rev. Lett., 48, 1559 (1982). Copyright 1982 by the American Physical Society. **c**) Single edge mode conduction in a Hall bar configuration for $\nu = 1$

As shown in figure 1.5b, the conduction in the edges is immune to back scattering from impurities resulting in a vanishing R_{xx}. These edge modes are therefore *dissipationless* causing the voltage drop along same edge to be almost zero leading to a vanishing R_{xx}. In Figure 1.5 c, such an edge state is shown for a Hall bar geometry for the case of $\nu = 1$.

The next obvious question is why the Hall resistance is quantized to these exact values independent of the material and size? The R_H is given by the precise values.

$$R_H = \frac{h}{ie^2} \qquad (1.5)$$

where $\nu = i$ and i takes on integer values. Landauer and Büttiker [12,13] formulated a theoretical framework in which each conducting edge state contributes e^2/h to the total conductance through the device. Such a derivation can be followed in detail from ref. [12,13]. Therefore, at $\nu = 2$, when the Fermi energy E_F crosses above the second spin split landau level, the total conductance contribution from the two conducting edge states is $2e^2/h$. The 4-wire Hall voltage measured will then be equal to $V_{xy} = Ih/ie^2$ where i is the number of conducting edge modes. The Hall resistance is then independent of the sample geometry and is given by $R_{xy} = \frac{h}{ie^2}$, dependent just on the fundamental constants.

1.2 Fractional Quantum Hall Effect

Soon after the discovery by von Klitzing, Tsui, Stormer and Gossard [3] observed a quantized Hall plateau at $\nu = 1/3$ and a minima in longitudinal resistance in a GaAs/AlGaAs sample as can be seen in Figure 1.6. The opening of a gap within a Landau level was unexpected in the single particle physics of the integer quantum Hall effect. With the observation of many other fractional states, it was soon realized that that the inter-electron Coulomb interactions play a significant role in determining these new ground states. With a brilliant insight, Robert Laughlin theorized a wavefunction for the newly observed fractional state which holds for states at $\nu = 1/m$ where m is an odd integer [4].

$$\Psi_{1/m}^{Laughlin} = \prod_{j<k}(z_j - z_k)^m \exp\left[-\frac{1}{4l_B^2}\sum_i |z_i|^2\right] \qquad (1.6)$$

where $z_i = x_i + iy_i$ is the complex coordinate of ith electron and $l_B = \sqrt{\hbar/eB}$ is the magnetic length which is a measure of the average distance between electrons

at any given magnetic field. In addition, the requirement of antisymmetry on the fermion wavefunction requires that m be an odd integer. This wavefunction describes the odd-denominator states at filling factor $\nu = 1/m$. However, many additional fractional states were observed at $\nu = p/q$ corresponding to rational fractions which could not be explained by Laughlin's wavefunction. As a result, a new theoretical framework was needed to explain these observations.
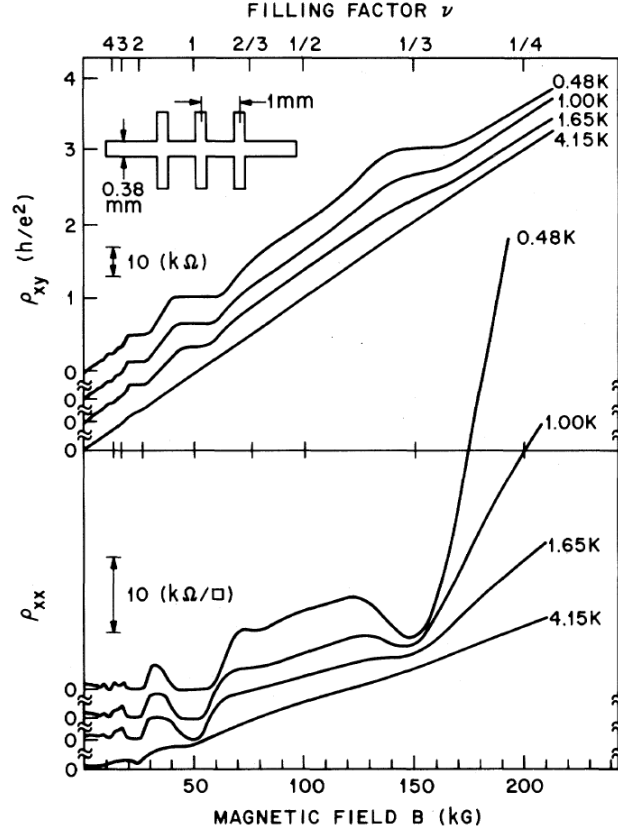
Figure 1.6. Original plot of the discovery of the first fractional state at $\nu = 1/3$. The Hall resistance is quantized to $3h/e^2$ and the longitudinal resistance nearly vanishes at about 150kG magnetic field. Reprinted figure with permission from D.C. Tsui, H.L. Stormer and A.C. Gossard, Phys. Rev. Lett., 48, 1559 (1982). Copyright 1982 by the American Physical Society.

It was the ingenious composite fermion theory proposed by Jain [5] that fit the Laughlin odd denominator states as well as the plethora of fractional states that were observed later. In this picture, each electron is seen as attached to an even number of
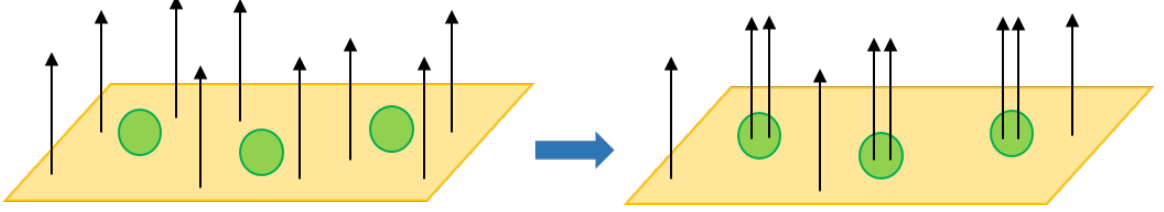
Figure 1.7. On the left is a representation of electrons at filling factor $\nu = 1/3$ where green circles denote the electrons and the quantized vortices are marked by black arrows. This is a strongly interacting system of electrons with three vortices for each electron. On the right, *Composite Fermions* in a reduced magnetic field with one vortex per CF. The CF filling factor is $\nu^* = 1$. This transformation maps a system of strongly interacting electrons to those of weakly interacting composite fermions.

magnetic quantized vortices ($\phi_0 = h/e$). An electron going in a closed path around a flux quantum acquires a phase of 2π. This union of an electron with even number of quantized vortices is known as a composite fermion (CF). Since some of the magnetic field is already tied up to the composite fermions, the *effective* magnetic field that these CFs see is reduced according to the following relation

$$B^* = B - 2n_s p \phi_0 \tag{1.7}$$

where p is an integer and n_s is the electron density. FQH states can then be viewed as integer Hall states of these composite fermions in the reduced effective field B^*. This formulation transforms the *strongly* interacting electrons to *weakly* interacting composite fermions (CFs) which form Λ levels similar to the Landau levels for electrons and well explains the sequence of observed incompressible states at

$$\nu = \frac{n}{2pn \pm 1} \tag{1.8}$$

In terms of these CFs, the $\nu = 1/3$ as seen in Figure 1.7 is equivalent to the $\nu = 1$ IQHE of electrons with one Λ level filled. The above picture is formulated in terms of electrons, however when particle-hole symmetry is exact, the same fractional states can be understood as being depleted of electrons or filled with holes. States at filling factor ν and $1 - \nu$ are then related by particle-hole symmetry and in this case the FQHS at 2/3 will be such an example.

1.2.1   N=0 Lowest Landau Level

The first fractional quantum Hall state at $\nu = 1/3$ was discovered [3] in the N=0 Landau level. With improvement in sample quality and lower electron temperatures achieved, the landscape in the N=0 level developed over the years.
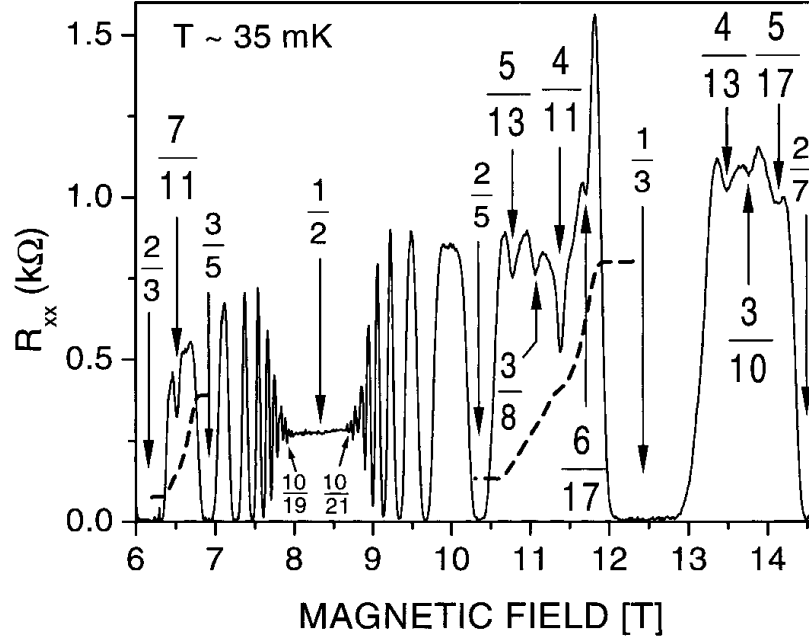
Figure 1.8. Magnetoresistance in the N=0 lowest Landau level in the filling factor range $2/3 < \nu < 2/7$ at 35mK. Prominent filling factors are marked by arrows. The dashed line shows the Hall resistance at 7/11 and 4/11. Reprinted figure with permission from W. Pan et al., Phys. Rev. Lett. 90, 016801 (2003). Copyright 2003 by the American Physical Society.

In Figure 1.8 such a rich array of fully developed fractional states are shown and many other developing states at filling factors such as 4/11, 5/13, 3/8 is shown in the plot at 35mK. Most of the Jain odd denominator sequence states and their particle-hole conjugates are observed in this region. Some exceptions and the recent proliferation of electron solids will be discussed in a subsequent section.

Composite Fermi sea at $\nu = 1/2, 3/2$

At half-filled Landau level, each electron attaches two quantized vortices resulting in a residual magnetic field $B^* = 0$. In the absence of CF interactions, the system at this filling factor is expected to behave similar to electrons at $B = 0$. Indeed, no fractional state is observed in the lowest Landau level (LLL) at half-filling. A classical Hall resistance with a non-zero longitudinal resistance is reported. Numerous experiments have been conducted around this filling factor so as to determine the cyclotron radius of composite fermions through geometric resonance and surface acoustic waves [30, 33, 34]. These experiments confirm the reality of composite fermions as legitimate particles.

However, unlike in the N=0 Landau level at 1/2 and 3/2 (in single subband occupation), fractional quantum Hall states have been observed at half-filling in the higher Landau levels at $\nu = 5/2, 7/2$ [21, 78]. In addition, anisotropic behavior is reported at higher half-fillings at $\nu = 9/2, 11/2, 13/2$ [75, 76]and so on. It reminds us that the physics at half filling is quite special.

Unconventional odd denominator fractional quantum Hall states

A large fraction of odd-denominator states in the lowest Landau level can be explained as the integer quantum Hall effect of weakly interacting CFs. However, there has been several reported odd denominator exotic composite fermion states that may result from the residual CF-CF interaction. The FQHS at $\nu = 4/11, 5/13, 4/13, 7/11, 5/17,$ and $6/17$ [29] in the N=0 Landau level do not belong the Jain

sequence of Eq. 1.8. For example, the states at 4/11 and 5/13 is understood as CF in the higher Landau level capturing additional flux vortices (due to the residual CF-CF interaction) to turn into higher order CF (^{4}CF) condensing into their own Λ levels [14].

1.2.2   N=1 Second Landau level

The second Landau level ($N = 1$) corresponding to the filling factor range $4 < \nu < 3$ hosts many important set of ground states which are not expected from the simple non-interacting CF picture. Unlike the lowest Landau level which hosts majority of the conventional odd-denominator Jain sequence states, the first *even* denominator FQHS at $\nu = 5/2$ [21] was reported here. Even though the first evidence of quantization was reported by Willett et al., the hallmark features of a FQHS were confirmed when a high mobility sample was cooled in a ^{3}He Immersion cell as shown in Figure 1.9 [77]. A deep minima in R_{xx} is accompanied by a well quantized plateau in R_{xy} at $2h/5e^2$. The FQHS state at this filling factor requires extremely low temperatures which were achieved by cooling the sample in the immersion cell.

Simple composite fermion picture expects a Fermi sea at this filling factor similar to 1/2 and 3/2. It was the motivation from the Bardeen-Cooper-Schreiffer theory of formation of Cooper pairs in superconductivity that lead Haldane and Rezayi to propose a wavefunction based on d-wave pairing of composite fermions [22]. Soon after, Moore and Reed proposed a Pfaffian wavefunction for the 5/2 state [23] explained in terms of triplet pairing of composite fermions. Numerical calculations by Morf [25] support the Moore-Read state. Interestingly, this state was predicted to support non-Abelian braiding statistics with a degenerate ground state [23, 35, 36]. Exchanging two non-Abelian particles results in a different ground state which was predicted to be useful for building topologically protected quantum computers [36–39]. Other candidate wavefunctions include Anti-Pffafian [26, 27] which is a particle-hole conjugate of the Pfaffian and likewise non-Abelian and the 331 state [24] which is predicted to be

Abelian. Therefore, the question on the true ground state at 5/2 and the non-Abelian statistics remain the subject of further novel experiments.

In addition to the 5/2 state, even denominator states at 7/2 [78] and 2+3/8 [79–81] have been reported. Recent experiments under extremely high hydrostatic pressure at 7/2 [28] indicate the importance of electron-electron interactions in transition between the isotropic FQHS and rotational symmetry broken anisotropic state. The $2 + 3/8$ on the other hand is much more fragile with energy gaps as small as 5mK, requiring extremely low electron temperatures. The interest in even denominator states has been renewed due to the recent observations of such states in graphene [82, 83] and ZnO [84].
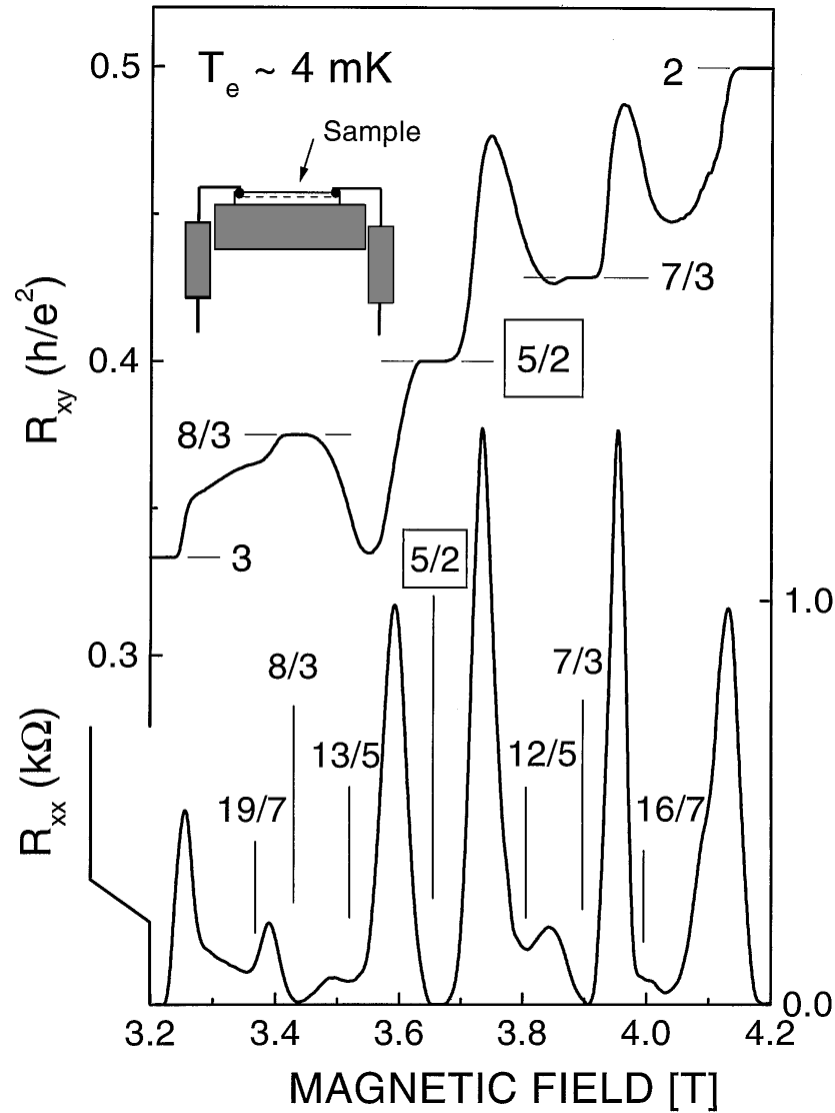
Figure 1.9. R_{xx} and R_{xy} in the second Landau level at T= 4mK. Well quantized fractional state at 5/2 is observed with several other developing states marked by their filling factor [77]. The Hall resistance is approaching the nearest integer values at some filling factors representative of reentrant states. Reprinted figure with permission from W. Pan et al., Phys. Rev. Lett. 83, 3530 (1999). Copyright 1999 by the American Physical Society.

Some of the odd denominator states in the second Landau level that are of different physical origin are the 2+2/5 [79] and the 2+6/13 state [80, 81]. Read and Rezayi

proposed a wavefunction in terms of paired parafermions applicable at the $\nu = 2+2/5$ state and its particle-hole conjugate at $2+3/5$ for which there is no clear experimental signature yet. In a later chapter, we discuss this state in light of our results in the competition between different ground states in the second Landau level. Interest in these FQHS arises from predictions of quasiparticles hosting Fibonacci anyons [86,87] which are expected to allow for universal quantum computation.

1.3 Electron Solids

In addition to the fractional quantum Hall states, another important consequence of the electron-electron interaction is the formation of solid phases. These phases stabilized by the long range interactions have distinct signature in transport measurements. In transport, it is dictated by insulating behavior which can be of two different types. The first case is when all the particles in the system are pinned by disorder leading to huge insulating peaks in R_{xx}. Such a case will be discussed briefly. Another possibility is for the particles in the partially filled Landau (Λ) for electrons (composite fermions) to be pinned and the transport exhibited by the underlying integer (fractional) state. Reentrant integer quantum Hall states is one such example. The schematic in Figure 1.10 shows some of these phases formed by electrons which have been observed while the corresponding states for the composite fermions have been predicted [145, 146] with few indications in experiments [129, 141, 143]. Solid phases with more than one particle localized at each lattice site as shown in Figure 1.10 (b) and (d) are the charged density ordered phases. Such a phase comprising of composite fermions has been predicted to exist theoretically [145] with no experimental evidence. However, we discuss such a possibility in Chapter 5. Such density modulation can also result in anisotropic transport such as the stripe or the nematic phases [44, 75, 76].
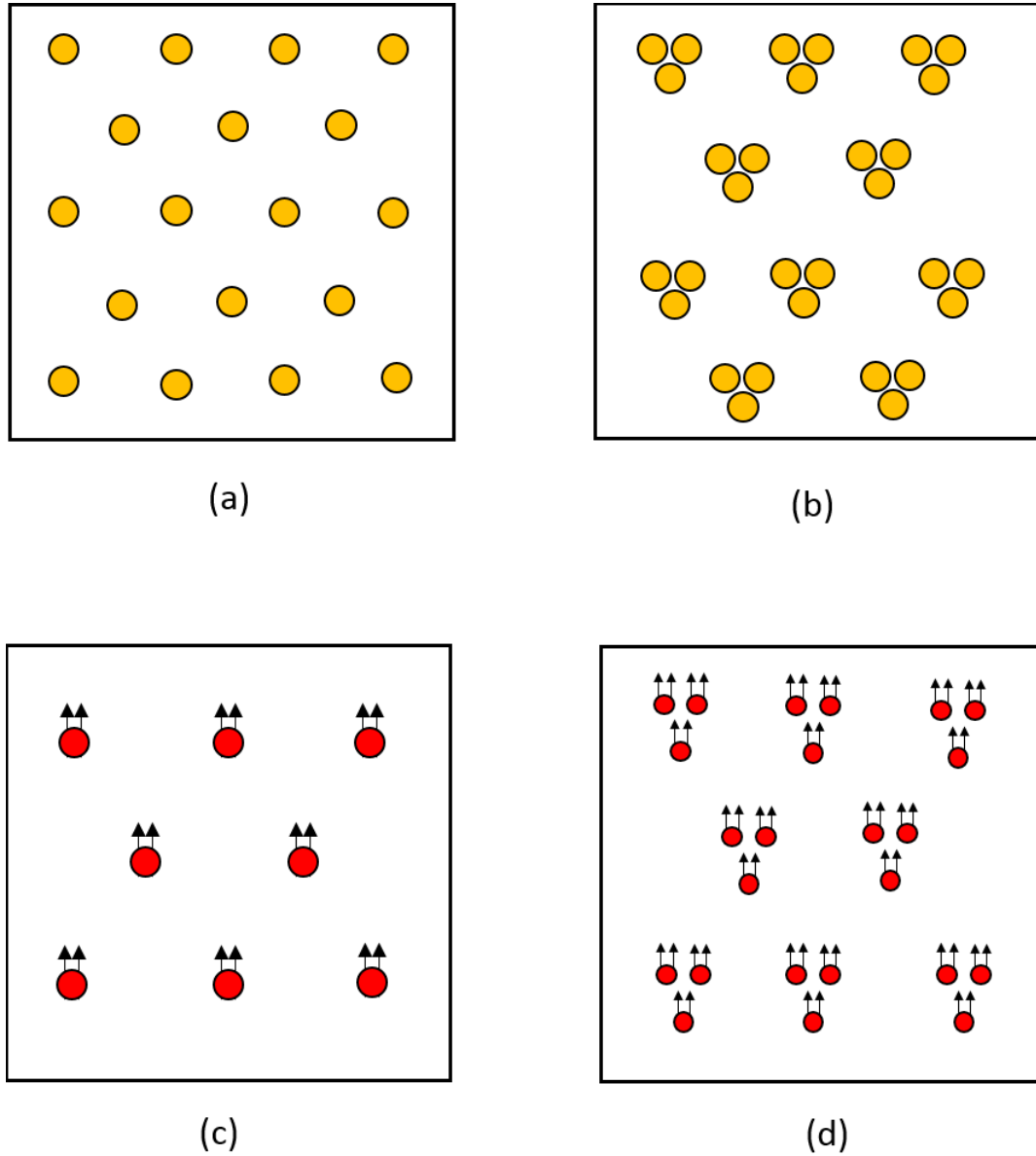
Figure 1.10. Schematic of the various possible solids. (a) Wigner crystal of electrons. (b) Bubble phase comprising electrons with three electrons per bubble in a triangular lattice. (c) Wigner crystal of composite fermions. (d) A bubble crystal of composite fermions with three ^{2}CFs (each electron is attached to two quantized vortices) localized at each lattice site.

1.3.1 Wigner Crystal and Exotic Electron Solids

The original motivation for the experiment by Tsui et al., was to look for the Wigner Crystal (WC) of electrons predicted to form at extremely high magnetic field [7]. This WC is expected to form when the Coulomb energy dominates the kinetic energy in the N=0 LL. Such an insulating crystal of electrons was indeed observed experimentally by Jiang et al. [138] near filling factor $\nu = 1/5$ as shown in Figure 1.11. As the filling factor approaches towards 1/5, a huge insulating peak in R_{xx} is observed near $\nu \sim 0.21$ (highlighted in yellow) with a subsequent observation of a well quantized state at $\nu = 1/5$ corresponding to four quantized vortices attached to each electron. For all filling factors less than 1/5, a rising exponential peak is reported which is highlighted in blue in the figure. Such a reemergence of insulating behavior below 1/5 and the highly insulating behavior at lower filling factors does not indicate single particle localization. Subsequent measurements in samples with varied disorder always exhibits this insulating characteristic which is taken as evidence for collective pinning of electrons by the small ubiquitous disorder potential [113]. The electrons are understood as forming a triangular lattice localized by the impurities in the sample. There has been recent theoretical work indicating that the crystal phase at these low fillings may not be a simple electron Wigner Crystal but may contain a series of composite fermion crystals [144, 147, 149] as depicted schematically in Figure 1.10 (c). A Wigner Crystal comprising of composite fermions with either two or four quantized vortices per electron has been considered theoretically with very little experimental evidence [141]. An elaborate review of these solids in GaAs system is well discussed by M. Shayegan in chapter 9 of the book in ref. [20].
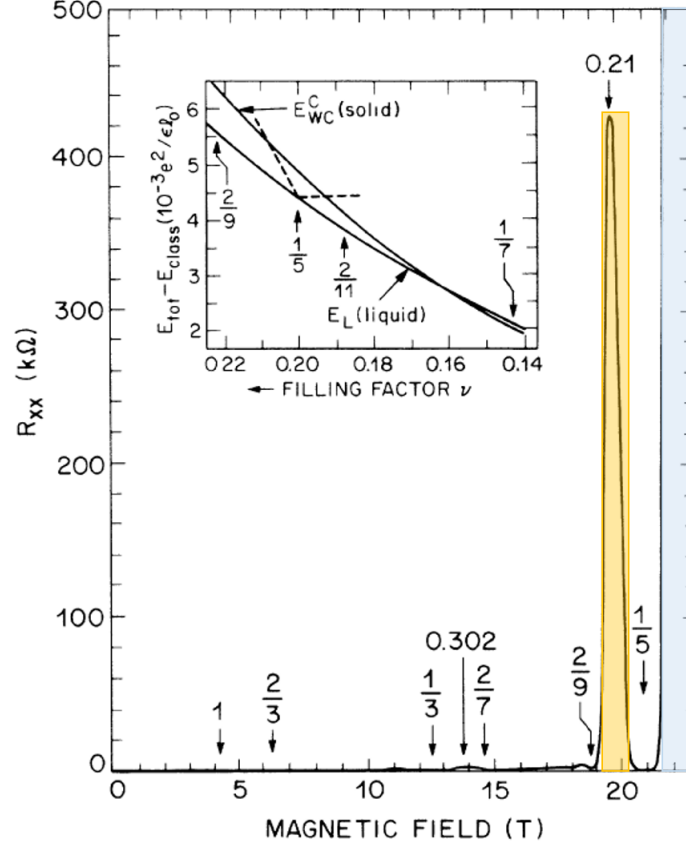
Figure 1.11. Observation of insulating behavior at extremely low filling factor near 1/5 shown on a plot of R_{xx} vs magnetic field at $T = 90$mK. The longitudinal resistance peaks at $\nu \sim 0.21$ which is highlighted in yellow and rises exponentially for all filling factors $\nu < 0.2$ (highlighted in blue). Inset shows a calculation of the energy of the solid and that of a liquid as a function of filling factor. Adapted from ref. [138]. Reprinted figure with permission from H.W. Jiang et al., Phys. Rev. Lett., 65, 633 (1990). Copyright 1990 by the American Physical Society.

1.3.2 Reentrant Integer Quantum Hall Effect

As seen in Figure 1.9, the Hall resistance landscape in the second Landau level looks quite different from that in the lowest Landau level. R_{xy} approaches the nearest integer value near while the longitudinal resistance almost vanishes. Such reentrance

is understood as collective localization of electrons often associated with the formation of electronic bubble phases [40, 43, 44]. These states were first reported in the third and higher Landau levels [75, 76] and subsequently observed in the second Landau level [78] as shown in Figure 1.12. Four reentrant states in the lower spin branch of the N=1 Landau level are observed with two on either side of the $\nu = 5/2$ FQHS. The experimental signature of reentrant states in electronic transport measurements is indicated by a vanishing $R_{xx} = 0$ and a quantized Hall resistance $R_{xy} = h/ie^2$ where $i =$ which is explicit from Figure 1.13 measured in a ^{3}He-Immersion cell [105] at an extremely low temperature of 6.9mK. With improvement in sample quality and lower electron temperatures achieved, these reentrant plateaus are very well developed. Unlike the integer states, these phases are observed centered at non-integral Landau filling factors. In the second Landau level, there is four such states in each spin branch
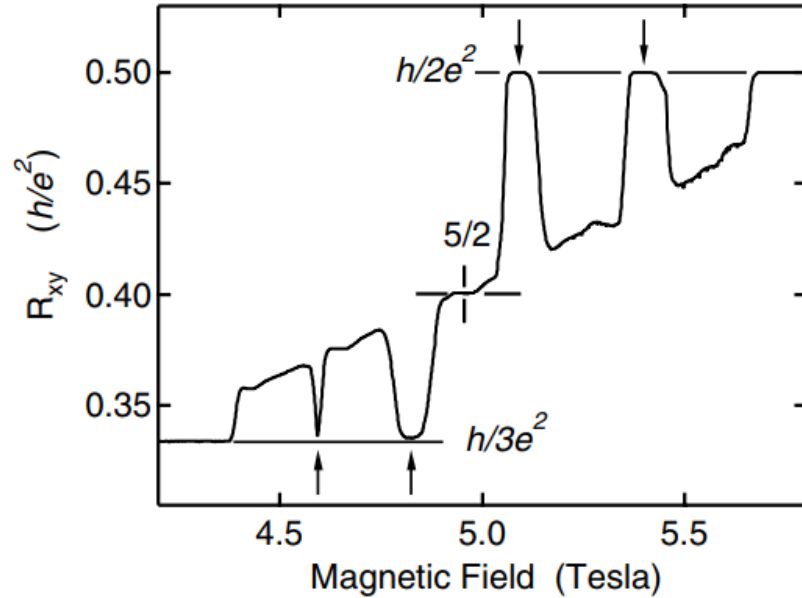
Figure 1.12. The first observation of RIQHS in N=1 Landau level with Hall resistance quantized to $h/2e^2$ and $h/3e^2$ for the four reentrant phases observed in the lower spin branch. Reprinted figure with permission from J.P. Eisenstein et al., Phys. Rev. Lett. 88, 076801 (2002). Copyright 2002 by the American Physical Society.

which appear at about 55mK. Each of these states develops with a precursor peak in magnetoresistance which has been extensively studied [88, 91].
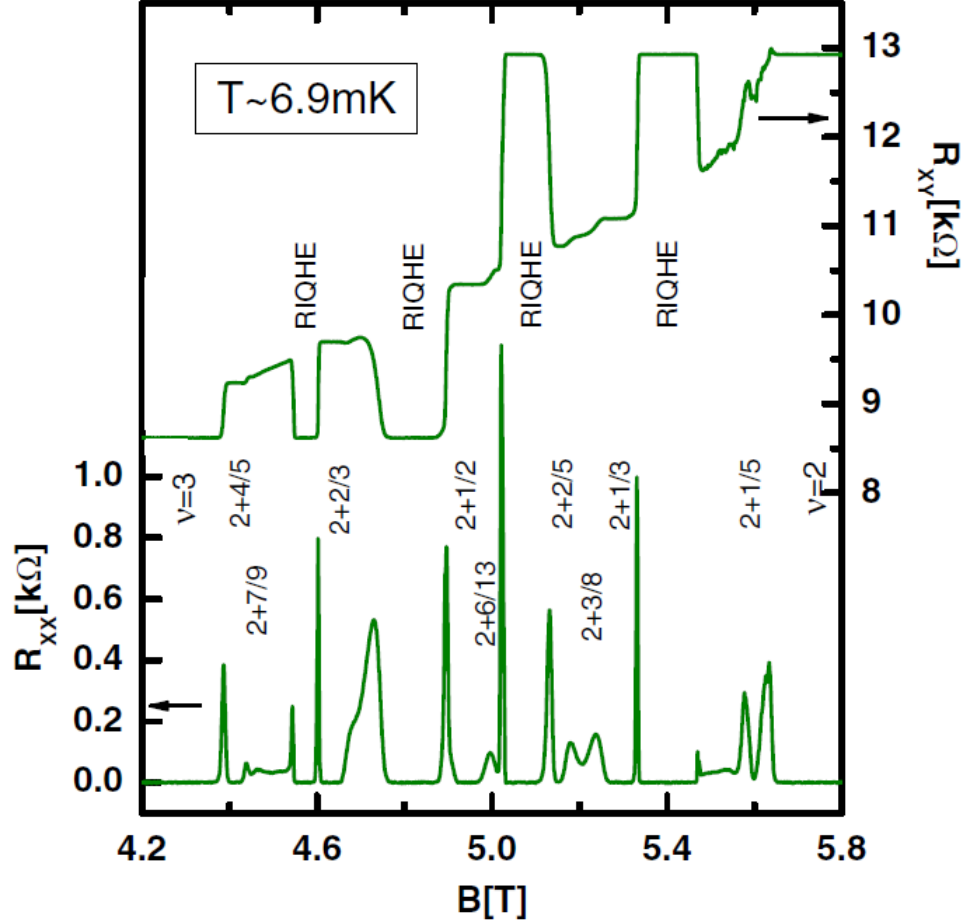
Figure 1.13. Magnetotransport in the lower spin branch of the second Landau level at an extremely low temperature of 6.9mK measured in a ^{3}He Immersion cell. The four RIQHS are marked. A deep minima at $\nu = 2 + 6/13$ attests to the high sample quality and low electron temperatures achieved [80]. Reprinted figure with permission from A. Kumar et al., Phys. Rev. Lett., 105, 246808 (2010). Copyright 2010 by the American Physical Society.

The above reentrant quantum Hall states in the higher Landau levels are associated with charge density ordered *bubble* phases. The electrons in the partially filled

Landau level condense into bubbles at each lattice site in a triangular lattice pinned by the disorder potential not contributing to conduction. The schematic in Figure 1.10(b) shows such a bubble phase of electrons even though the number of electrons per site is a topic of current interest. Such solids exhibit isotropic transport unlike the nematic phases which break rotational symmetry [40, 43, 75, 76]. Various experiments have been performed to study characteristics of these bubble phase including their electrical breakdown [45–50] which leads to a transition from an insulating to a conducting state pointing to the depinning of the charge density waves (CDW) and surface acoustic wave experiments [51, 52] which highlight the attenuation from such solid phases.

Microwave Absorption and Pinning Resonance Experiments

The existence of electron solids interpreted in terms of a crystal of electrons pinned by the small disorder potential has been verified by another experimental technique. The sample is excited at microwave radiation of about 1GHz which is absorbed and the response of the real part of conductivity $Re[\sigma_{xx}]$ is measured as a function of frequency f. This technique is particularly useful to study the Wigner Solids in the flanks of integer plateaus away from exact filling when there is dilute population of quasiparticles in the next excited Landau level [115, 116]. In Figure 1.14, such resonances in the microwave spectrum near $\nu = 1$ is shown with clear resonance indicating a solid phase. The frequency of the resonance f_{pk} yields information about the underlying disorder potential strength and correlation length [55]. Pinning resonances of Wigner Crystal [117], charge density waves including electronic bubble phases in the higher Landau levels [55, 56] as well as the stripe phases near half fillings [57] has been measured.
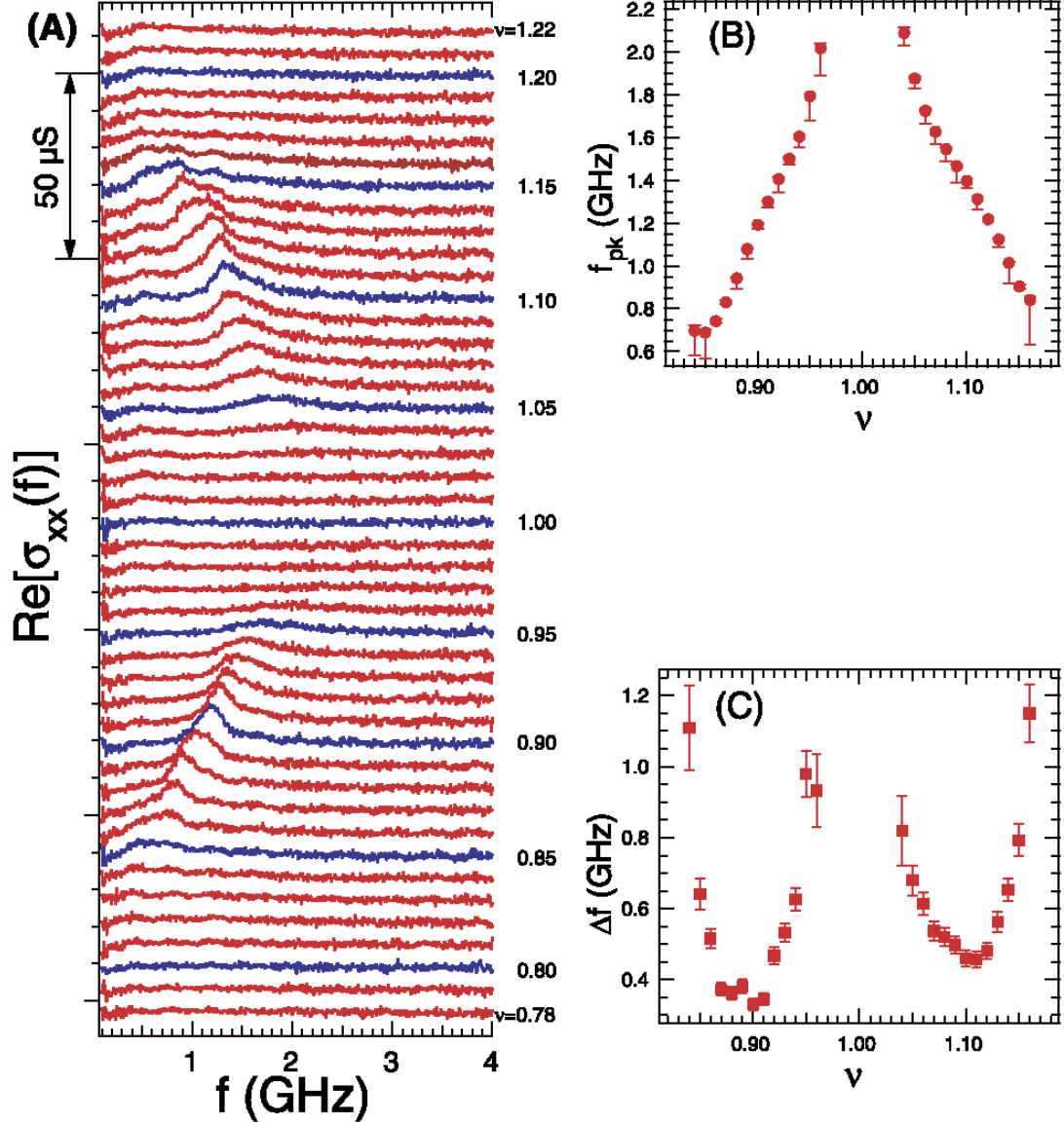
Figure 1.14. The observation of microwave resonances near the integer plateau at $\nu = 1$ [115]. (A) The conductivity response is measured as a function of frequency at different filling factors and each trace is offset for clarity. Figures (B) and (C) show the peak frequency f_{pk} and Δf as a function of the electron filling factor. Reprinted figure with permission from Y.P. Chen et al., Phys. Rev. Lett., 91, 016801 (2003). Copyright 2003 by the American Physical Society

1.4   Conclusion

Quantum Hall effect is indeed a hallmark phenomena leading to emergence of rich physics driven by interactions of electrons in two dimensions. The toplogical states as well as the Landau charge order phases are a manifestation of the emergent behavior. As discussed above, the charge density waves predicted to form in the higher Landau levels give rise to competing phases in the second Landau level. In the subsequent chapters, I willl discuss some of our recent results which exhibit novel ordered phases of electrons and composite fermions in the lowest Landau level.

2. EXPERIMENTAL TOOL SET

The physics of the fractional quantum Hall effect is based on restricting motion of electrons to two-dimensions. Molecular-beam epitaxy is used to grow these very high mobility samples that I will briefly describe. To study some of the insulating phases that I have described, we then need to cool these samples to extremely low temperatures in a strong magnetic field. I will then describe the essential working of a dilution refrigerator used to achieve such temperatures equipped with a super-conducting magnet. In addition, the He-3 immersion cell was used for some of the measurements in the second Landau level to thermalize the electrons to extremely low and stable temperatures.

2.1 Two-dimensional electron gas and Molecular Beam Epitaxy

The advancement in technology leading to confinement of electrons in reduced dimensions has been a cornerstone of modern condensed matter research. The quantum mechanical effects at play have lead to the observation of novel physics such as the fractional quantum Hall effect discussed. The recent proliferation of many such available semiconductor host systems for 2DEGs include AlAs/GaAlAs [58], Si/SiGe [60], Ge/SiGe [61,62], ZnO/MgZnO [63], CdTe/CdMgTe [59]. Advancement of such platforms is enhanced with pioneering work in graphene [65] and other layered materials such as transition metal dichalcogenides [66] and black phosphorus [67]. Despite the recent observations of FQHE in other material hosts such as graphene [68] and ZnO [69], GaAs/AlGaAs quantum wells remain one of the cleanest systems with electron mobilities of the order of $\mu = 36$ million cm^2/Vs [72] which have resulted in many new phases exclusive to GaAs.

The importance of molecular beam epitaxy (MBE) for growth of such high mobility samples cannot be overstated. The sample mobility achieved in these heterostructures is one of the highest with continued improvement as shown in Figure 2.1. MBE is a ultra high-vacuum (UHV) evaporation technique which allows the for the thermal evaporation of high quality thin-films of materials one layer at a time.
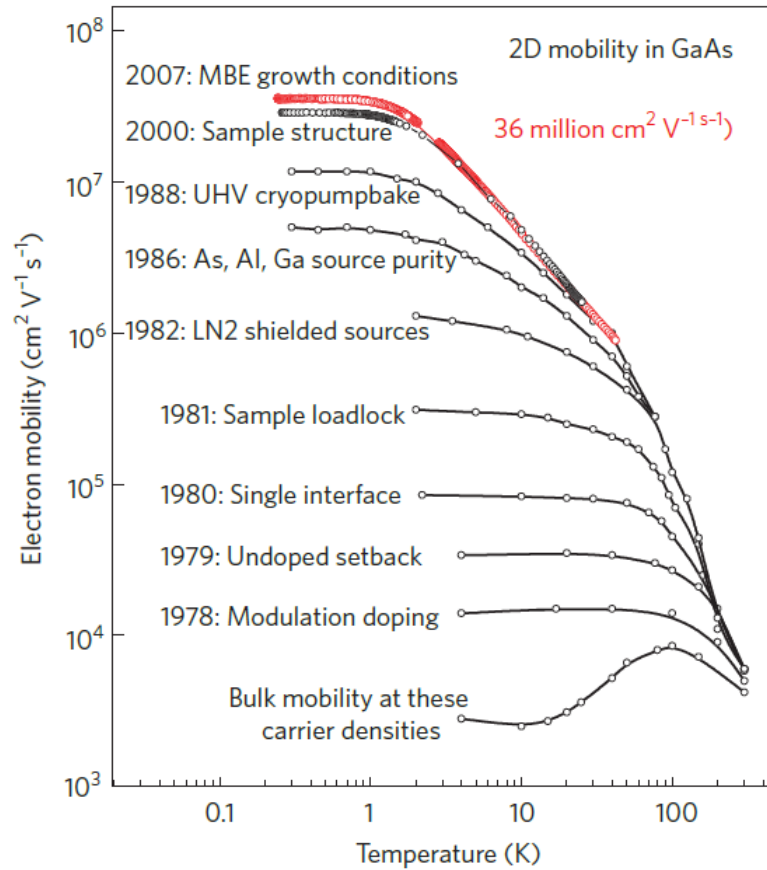
Figure 2.1. This shows the improvement in quality of 2DEGs in GaAs/AlGaAs measured in terms of sample mobility over several decades [72]. Reprinted figure with permission from D.G. Schlom and L.N. Pfeiffer, Nature Materials 9, 881 (2010). Copyright 2010 by Nature Materials.

The next important tool for growth of highest quality samples is the sample structure and the choice of materials. The mobility given by $\mu = e\tau/m^*$ is naturally high

for GaAs due to its low effective mass m^*. To confine the motion of electrons, two semiconductors with difference in bandgap are stacked together trapping electrons from the donor ions in a potential well. AlGaAs and GaAs make a good combination due to very similar lattice constants causing minimal strain during layered growth resulting in reduced interfacial scattering [19]. Such a sandwich of GaAs surrounded by AlaGaAs as shown in Figure 2.2. The content of Al is controlled for optimizing the structure of $Al_xGa_{1-x}As$ where x is the concentration of Al with $x = 20 - 30\%$ for optimal results [19, 70, 71].
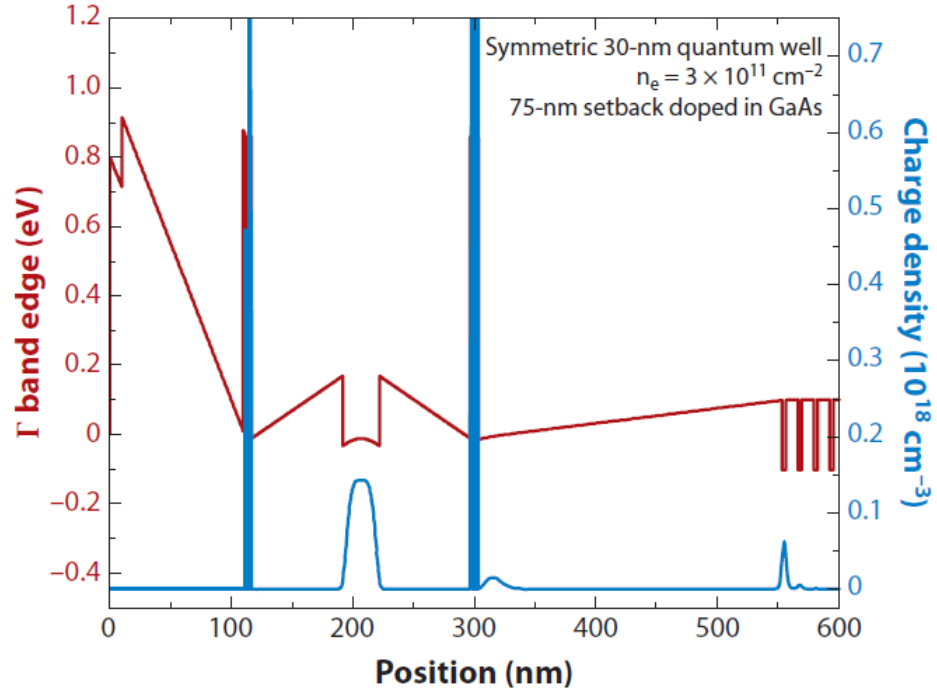
Figure 2.2. The conduction band minimum of $GaAs/Al_xGa_{1-x}As$ (red) growth profile and the electron density (blue) of a quantum well structure. The Si dopants are grown into narrow quantum wells (3nm) on both side of the 30 nm GaAs well which are indicated by peaks in charge density profile. The main GaAs quantum well with the 2DEG is at about 200 nm from top surface (0 on the scale). From ref. [71].

An important aspect of doping (Si for n-type) these high quality structures is a technique called *modulation doping* [70], which reduces scattering with donor ions by placement of donor ions at a distance of 50-100 nm away from the quantum well. These doping quantum wells are evident from the peaks in charge density in Figure 2.2. Such a scheme has revolutionized the contemporary mobilities to the order of 10^7 million cm^2/Vs.

To measure transport of the 2DEG underneath (200 nm below the surface), In/Sb contacts are placed at the edges of the cleaved wafer which is usually a square piece of 5mm by 5mm. These indium contacts are then annealed in a homemade rapid thermal annealer at 450° for a few minutes within a chamber filled with forming gas composed of H$_2$ and N$_2$.

2.2 Dilution Refrigerator

The dilution refrigerator based on the mixing of dilute ^{3}He in a concentrated ^{4}He is a closed cycle system most commonly used to achieve milliKelvin (mK) temperatures. The cooling based on the phase-diagram of these two isotopes of helium is at the heart of the working of this refrigeration technique with many other essential components. To understand the cooling mechanism achieved with a mixture of ^{3}He and ^{4}He, we look at the phase diagram of temperature vs mixing concentration as shown in Figure 2.3. At a temperature of about ∼ 0.9K, the liquid undergoes a phase separation into a concentrated He-3 rich phase and a dilute phase rich in He-4. The cooling power relies on the entropy of mixing of the two isotopes. The He-3 is distilled away from the mixture causing He-3 atoms to move from the concentrated phase to the dilute phase resulting in absorption of heat and thus cooling. In order to run this in a closed cycle, the evaporated He-3 is returned to the mixture via several steps which will be discussed next.

A schematic of the dilution fridge is shown in Figure 2.4. The 4K stage of the refrigeration is achieved by inserting the experimental probe in He-4 liquid. However,
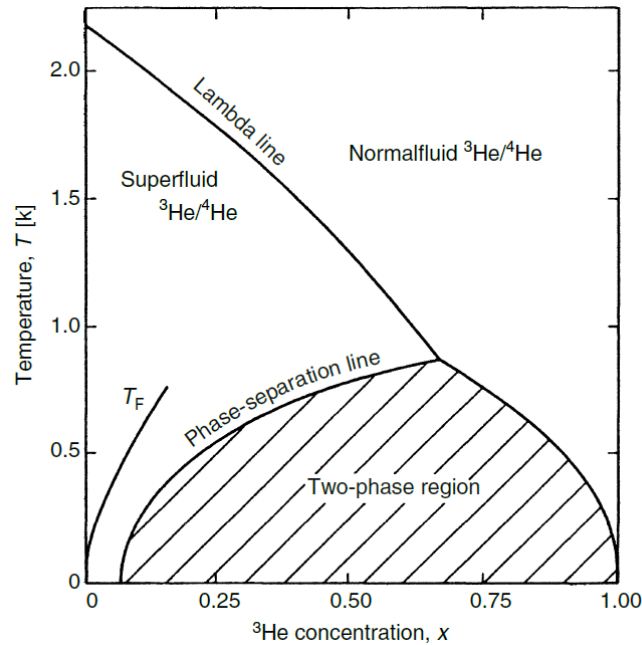
Figure 2.3. The temperature vs concentration phase diagram of liquid ^{3}He -^{4}He mixture. Plot from ref. [15]

the incoming gaseous mixture cannot be liquefied with a 4K stage as He-3 condenses at 3.4K. Therefore, a 1K pot stage is setup by pumping on the helium liquid which is supplied continuously from the surrounding helium bath. This is the stage where the condenser is located at which point the mixture first condenses into a liquid. There is a number of heat exchangers which cool the incoming mixture before it reaches the mixing chamber. The phase boundary is formed inside the mixing chamber which is the coldest stage in the system. A stage called the still is where the He-3 gets pushed due to osmotic pressure causing the He-3 atoms to cross the phase boundary and thus cooling the system. The mixing chamber is heat sunk very well to a copper tail which houses an assembly with the sample shown in dark tan in the Figure 2.4. The sample sits at the center of the bore of the superconducting magnet. The magnet is a single coil solenoid made with Niobium alloy with a superconducting transition below 7K
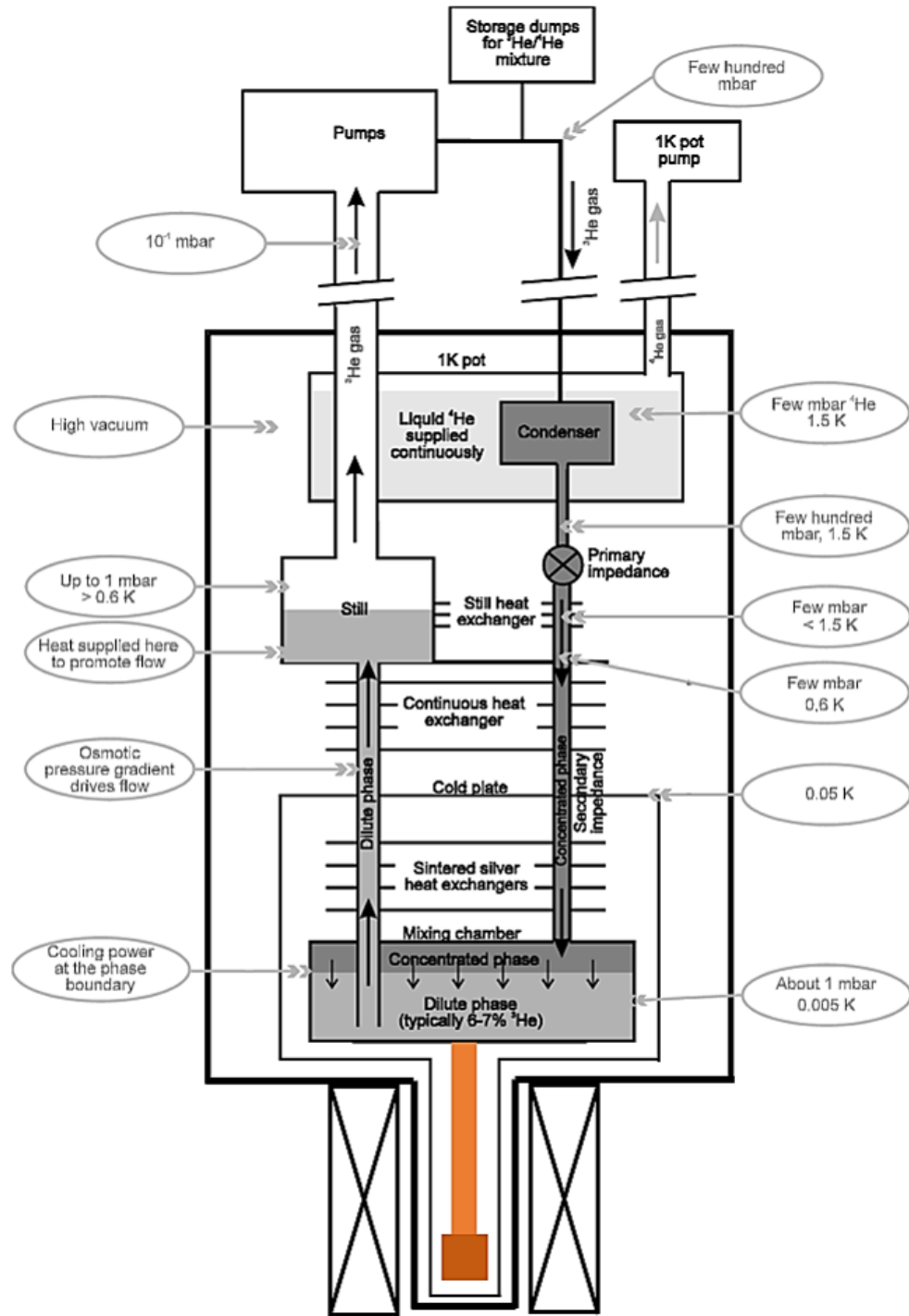
Figure 2.4. Schematic of a dilution refrigerator showing the various cooling stages. The sample (dark tan) is attached to the mixing chamber via a copper tail shown in tan. The sample sits at the center of the bore of a superconducting magnet. Adapted from ref. [74]

and therefore is always kept cold in the helium bath at 4K. The coils of the magnet can carry upto 100 A of current without dissipitation.

The temperature of the mixing chamber is monitored with a homemade resistive thermometer which is sensitive to temperatures down to 5mK. There is several other components to the functioning of the dilution refrigerator which include cold traps at 77K and 4K to absorb any air while the mixing is circulating in a closed cycle. It is extremely important to keep an eye for any leaks as air leaks can cause the system to warm up or hamper the movement of the mixture by creating icy obstructions.

2.3   He-3 Immersion cell

More often, even when the mixing chamber reaches single digit mK temperatures, the electrons in the two-dimensional electron gas are much warmer due to the Kapitza thermal resistance [73]. To resolve this issue, a He-3 immersion cell [105] was designed for ensuring electron thermalization to the base temperature of our dilution refrigerator. The cell is made of a polycarbonate body with a threaded cap as shown on the left in Figure 2.5. It is filled with He-3 liquid which provides excellent thermal conductivity at mK temperatures and enables viscometry based temperatures measurements. A schematic of the inside of the cell is shown on the right in Figure 2.5. The sample sits on a copper base with silver sinters filled heatsinking wires for increased area of thermal contact. A quartz tuning fork in red is used for temperature measurements based on the temperature dependent viscosity of He-3. The challenge for making this kind of setup is for it to be completely leak-tight.

Some of the data in the second Landau level that I discuss in the next chapter was taken with the immersion cell. Electron temperatures as low as 6.9mK were achieved which have been instrumental in observation of some very fragile fractional states such as 2+3/8 and 2+6/13 [80].
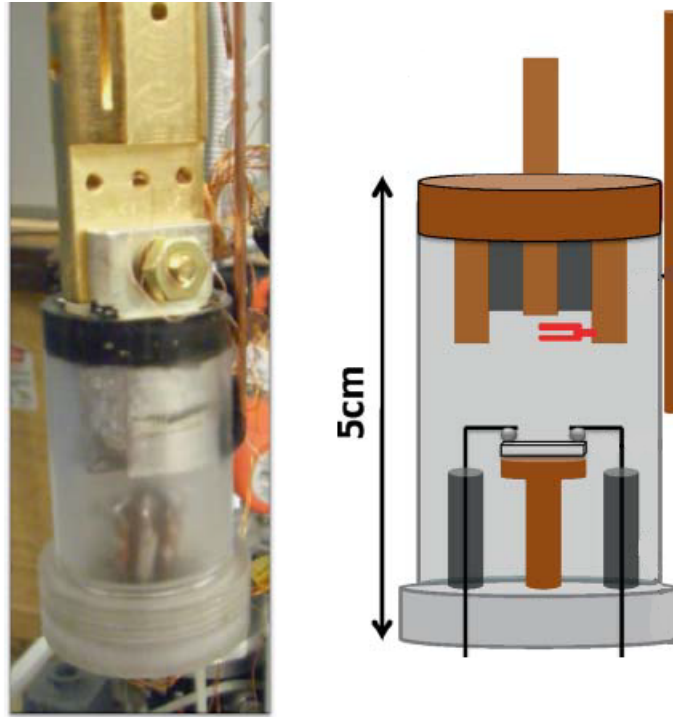
Figure 2.5. Left: Picture of the Immersion cell mounted on the mixing chamber tail. Right: Schematic of the cell which shows the platform where the sample sit and connected to the silver sintered wires. The tuning fork is shown in red which is used for thermometry. The gray area inside is filled with He-3 liquid. Reprinted figure with permission from N. Samkharadze et al., Rev. Sci. Instrum. 82, 053902 (2011). Copyright 2011 by the American Institute of Physics.

2.4   Copper Tail Mount

The results presented in chapter 3 were acquired with the sample mounted in the immersion cell. However, experiments reported in chapter4 and 5 were performed with the sample placed on a copper tail as shown in Figure 2.6. We measured two samples in this cooldown with a LED for each one used for illumination at 10K and for mK illumination discussed in chapter 4. The samples were attached to the copper base with vacuum grease which provides a good thermal and mechanical contact. The samples are cooled via the copper wires attached with indium solder for making connection to the ohmic contacts seen as silver spots on the sample perimeter. The
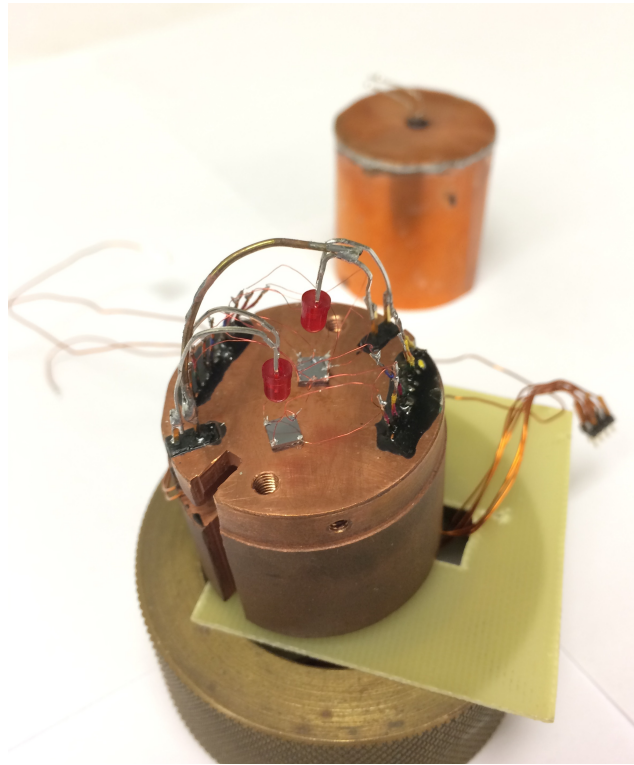
Figure 2.6. A picture of the copper sample mount with two samples attached. Two red light emitting diodes were used for low-temperature illumination. The electrical wires soldered to the sample are attached to a header on the other end. A copper radiation shield cap was attached to the copper tail before mounting in the fridge.

two samples used in the study presented in this thesis will be denoted as Sample 1 with electrons confined is a 30nm quantum well, electron density $n = 3.0 \times 10^{11}/\text{cm}^2$ and mobility $\mu = 32 \times 10^6 \text{cm}^2/\text{Vs}$. Sample 2 from a different wafer has similar characteristics in a 30nm quantum well with electron density $n = 3.0 \times 10^{11}/\text{cm}^2$ and mobility $\mu = 28 \times 10^6 \text{cm}^2/\text{Vs}$.

2.5   Conclusion

The essential tools for exploring the quantum effects of two-dimensional electron systems needs both the state-of-art growth techniques and the cryogenic development of the dilution refrigerator. With the novel-design of the He-3 immersion cell necessary for achieving the lowest electron temperatures, we see some phenomenal states in the second Landau level. In the rest of the document, I will discuss the results obtained with this experimental toolkit.

3. ELECTRON SOLIDS IN THE SECOND LANDAU LEVEL AND THEIR COMPETITION WITH FRACTIONAL QUANTUM HALL STATES

As described previously, the second Landau level witnesses numerous fractional quantum Hall states (FQHSs) [21, 77–81]. Several of these FQHSs are thought to have topological order and exotic quasiparticle excitations which cannot be realized in the lowest Landau level [3]. Apart from the most well-known even denominator state at $\nu = 5/2 = 2 + 1/2$ [21, 77], which is believed to belong to the Pfaffian universality class and to host Majorana-like excitations [23, 85], the $\nu = 2 + 2/5$ is another FQHS of interest [79] as it is a candidate hosting Fibonacci anyons [86, 87]. In addition to the many interesting FQHSs, the second Landau level also hosts a set of traditional Landau phases with charge order. Examples of such charge order are the eight the electronic bubble phases [40, 78, 88] that are observed. Therefore, the region of the second Landau level stands out among other Landau levels in a prominent display of phase competition between two classes of different phases: FQHSs and charge ordered phases [79]. As a result, there have been reports of weak local minima in the magnetoresistance at $\nu = 2 + 3/5$, $2 + 3/7$, $2 + 4/9$, $2 + 5/9$, $2 + 5/7$, and $2 + 5/8$ which have opened the possibility of fractional quantum Hall states at these filling factors. These features may be a result of a competition between the reentrant states near these filling factors and fractional states developing.

In this chapter, I will discuss our study of the temperature dependence near these features, where we find that these cannot be associated with fractional quantum Hall states; instead they originate from magnetoresistive fingerprints of the electronic bubble phases. We found only two exceptions: at $\nu = 2 + 2/7$ and $2 + 5/7$ where there is evidence for incipient fractional quantum Hall states at intermediate temperatures.

As the temperature is lowered, these fractional quantum Hall states collapse due to a phase competition with the nearby bubble phases.

3.1 Temperature evolution of magnetoresistance in the Second Landau Level

In many experiments, data in the second Landau level on the highest quality samples exhibit a consistent set of fully developed FQHSs at $\nu = 2 + 1/2$, $2 + 1/3$, $2 + 2/3$, $2 + 1/5$, $2 + 4/5$, and up to four bubble phases in the filling factor range $2 < \nu < 3$. In addition, in setups attaining the lowest temperatures, many developing FQHSs are observed at $\nu = 2+3/8$ [79–81,91,93–97,133], $2+6/13$ [80,81,91,93,94,133], $2+2/9$ [91], $2+7/9$ [81,91,96] and $2+2/7$ [79,95,98,133]. However, a careful review of the literature reveals several additional minima in the longitudinal resistance, such as the ones at $\nu = 2+5/8$, $2+5/7$ in Ref. [133], $\nu = 2+3/5$, $2+3/7$, $2+5/7$, $2+4/9$, $2 + 5/9$, $2 + 5/8$ in Ref. [95], and $\nu = 2 + 4/9$, $2 + 5/9$, $2 + 5/7$ in Ref. [99]. Even though these minima develop at filling factors compatible with FQHSs, they could not be associated with FQHSs either due to of lack of Hall data [95, 133] or because the quantization of the Hall resistance was inconsistent with that of a FQHS [99]. Furthermore, with the exception of $\nu = 2 + 5/8$, other experiments report bubble phases at either lower electron temperatures and/or in higher quality samples at the filling factors of these additional minima [79–81, 91, 94, 96, 97].

There may be several reasons for the development of the above-mentioned additional local minima in R_{xx} in certain experiments but of bubble phases in others. First, different growth parameters of samples alter the electron-electron interaction that may result in a drastically different set of ground states. It is thus possible that, with improvement in sample quality, the signatures seen in Refs [95, 99, 133] develop into well quantized FQHSs. Secondly, the available data may indicate a temperature-driven phase competition between the FQHSs and bubble phases. Indeed, there are well-known FQHSs present at intermediate temperatures, which give way to a charge-

ordered phase at the lowest accessible temperatures. A few examples of such FQHSs are at $\nu = 1/7$ [100,101] and 2/11 FQHSs [101] in the lowest Landau level, $\nu = 4+1/5$ and $4 + 4/5$ in the third Landau level [102], and $\nu = 2 + 2/7$ in the second Landau level [79]. Of these, the FQHSs observed at intermediate temperatures in the second and third Landau levels transition into bubble phases as the temperature is lowered.

Here we examine whether the earlier seen minima in R_{xx} that could not be associated with a FQHS also develop in the second Landau level of a high quality GaAs/AlGaAs sample. We examine previously unavailable detailed temperature dependence to observe these phases at intermediate temperatures.

Sample 1 under study is a symmetrically doped 30nm quantum well sample with electron density $n = 3.0 \times 10^{11}/\text{cm}^2$ and mobility $\mu = 32 \times 10^6 \text{cm}^2/\text{Vs}$. Following the procedure described in the Supplement of Ref. [104], the sample state was prepared by a low temperature illumination with a red light emitting diode. The sample is mounted in a He^3 immersion cell which ensures electron thermalization to the base temperature of our dilution refrigerator and enables a convenient setup for temperature measurement through quartz tuning fork viscometry [105]. The excitation current used for transport is 2nA.

Figure 3.1 captures the temperature evolution of magnetoresistance traces in the second Landau level in the temperature range between $T = 59$ and 6.9 mK. We observe several FQHSs among which the most prominent ones are at $\nu = 2 + 1/2, 2 + 1/3, 2 + 2/3, 2 + 1/5$, and $2 + 4/5$. Traces of Fig.1 appear very different from those measured in the lowest Landau level [9] due to the presence of the reentrant integer quantum Hall states [78,88]. These reentrant states are believed to be exotic electronic solids called the bubble phases [40, 75, 76]. The bubble phases we observe are marked by yellow shading in Fig.1. At the lowest temperatures, the bubble phases are signaled by a vanishing R_{xx} and the Hall resistance R_{xy} quantized either to $h/2e^2$ or $h/3e^2$ (not shown) [78]. Furthermore, these reentrant states are delimited by two distinct peaks in R_{xx}, which can be seen near the edges of the shaded areas [88] in Fig.1. The size of such peaks may exceed 1.8 kΩ, therefore, dominating the magnetoresistive landscape.
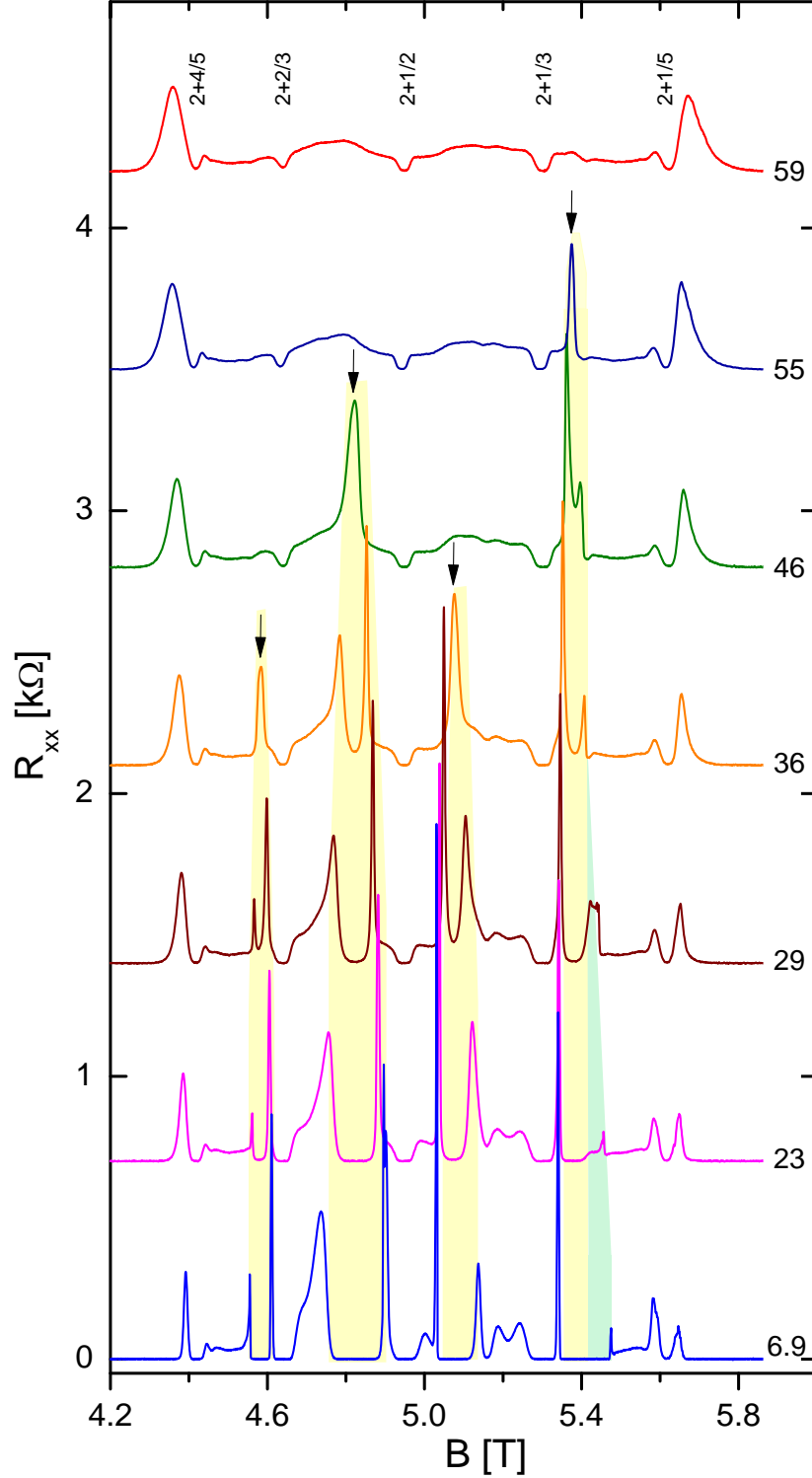
Figure 3.1. Waterfall plot of the magnetoresistance in lower spin branch of the second Landau level ($2 < \nu < 3$). Filling factors of the five most prominent FQHSs are shown. The shaded areas mark the bubble phases present. Arrows indicate precursors of the bubble phases. Numbers on the side show the measured temperatures in mK. Reprinted figure with permission from V. Shingla et al., Phys. Rev. B 97, 241105(R) (2018). Copyright 2018 by the American Physical Society.

It was found that as the temperature is raised, the two peaks encompassing a bubble phase first merge into a single peak and this single peak then disappears as the temperature is increased further. As the appearance of these singular peaks at the highest temperature indicates the first signature of the bubble phases, they can be thought of as the precursors of the bubble phases. In Fig. 3.1, there are several examples marked by vertical arrows of these precursor peaks, such as the one at $B \simeq 5.37$ T in the $T = 55$ mK trace. At lower temperatures, near $B = 5.37$ T there are two distinct bubble phases, which will be discussed later.

3.2   The question of a fractional quantum Hall state at $2 + 3/5$

We first focus at filling factors related by particle-hole conjugation $\nu = 2 + 3/5$ and $2 + 2/5$. Interest in these quantum numbers stems from proposals and numerical evidence that these FQHSs have a unique topological order supporting non-Abelian anyons of the Fibonacci type [86, 87]. Features in magnetotransport at these two filling factors were first tentatively associated with FQHSs in Ref. [77]. However, no quantized Hall resistance was observed; the Hall resistance instead had features which were later attributed to the bubble phases. A fully developed $\nu = 2 + 2/5$ FQHS was observed in Ref. [79] and it is now routinely measured [79–81, 91, 93–98, 133]. In contrast to the observations at $\nu = 2 + 2/5$, at $\nu = 2 + 3/5$ no FQHS was detected in most experiments [79–81, 91, 93, 94, 96–98, 133]. The filling factor $\nu = 2 + 3/5$ often falls very close to the bubble phase $R2c$ instead. We are aware of only one work, in which a concave feature in R_{xx} was seen at $\nu = 2 + 3/5$ [95] at a temperature of $T = 36$ mK. We note that results in wide quantum wells are qualitatively different; we defer discussing these results to a later paragraph.

In Fig. 3.2, a magnified view of the $T = 6.9$ and 59 mK traces is shown. We focus on the $T = 59$ mK trace as this is the lowest temperature at which there are no noticeable features of the bubble phases. On this trace, we marked several filling factors of interest: the most prominent FQHSs at $\nu = 2+1/2, 2+1/3, 2+2/3, 2+1/5$,
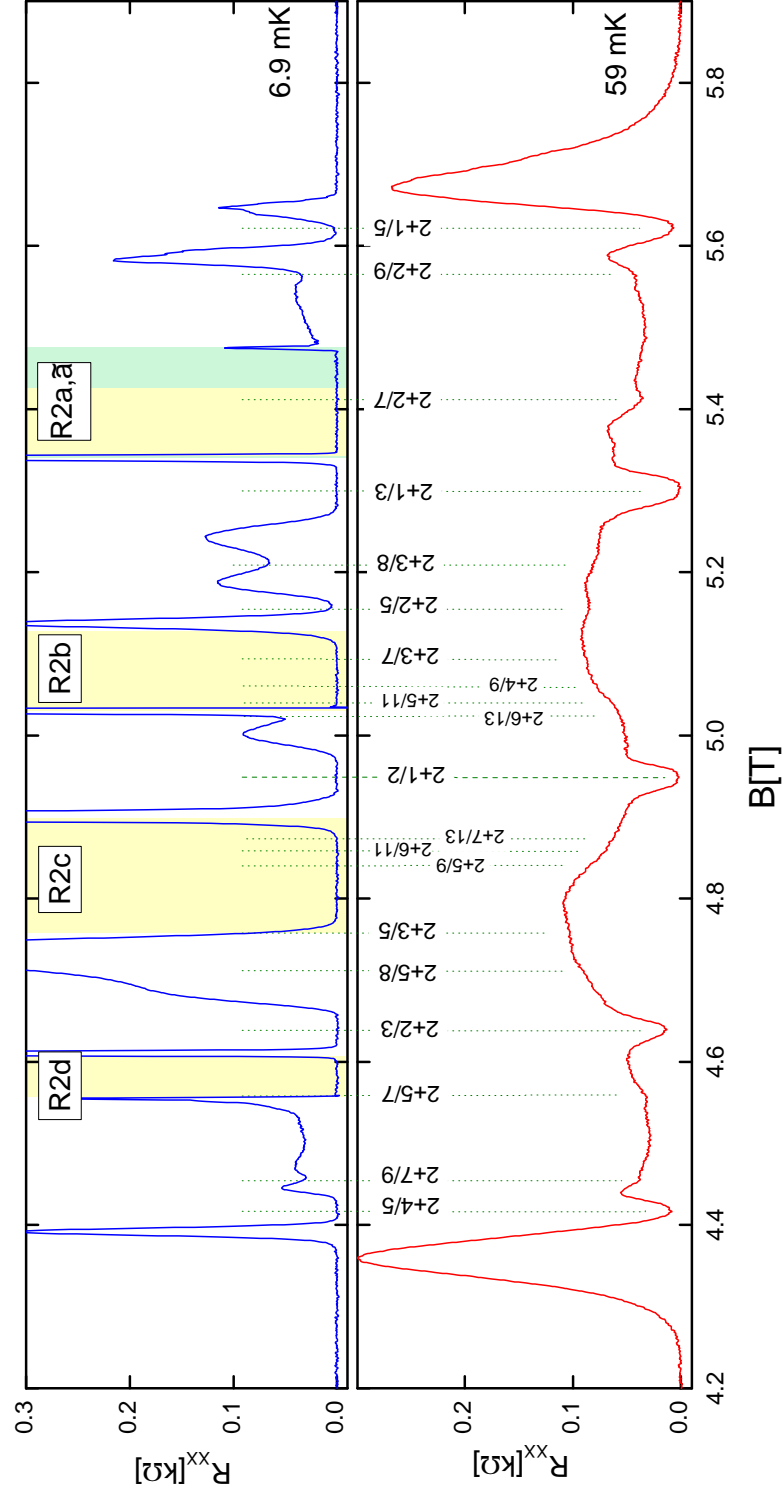
Figure 3.2. A magnified view of the magnetoresistance at $2 < \nu < 3$ as measured at $T = 59$ mK and 6.9 mK. The various filling factors of interest are marked by vertical lines. The shaded areas are bubble phases. Reprinted figure with permission from V. Shingla et al., Phys. Rev. B 97, 241105(R) (2018). Copyright 2018 by the American Physical Society.

and $2 + 4/5$. Additional features are seen at several other filling factors such as relatively narrow depressions in R_{xx} at $\nu = 2 + 2/5$, $2 + 2/7$, $2 + 2/9$, $2 + 7/9$, $2 + 5/7$ and $2 + 3/8$. Other features are broader, such as those near $\nu = 2 + 3/5$ and in the vicinity of $\nu = 2 + 1/2$, on each side. Of these features, only some of them develop into a FQHS at lowest temperature of $T = 6.9$ mK. Indeed, in the $T = 6.9$ mK trace, we identify fully developed FQHSs at $\nu = 2 + 1/2$, $2 + 1/3$, $2 + 2/3$, $2 + 2/5$ and less developed FQHSs at $\nu = 2 + 6/13$, $2 + 2/9$, $2 + 7/9$, and $2 + 3/8$. In the following, we will examine the temperature dependence of the additional features of R_{xx} shown in the $T = 59$ mK trace of Fig.2. We will search, in particular, for signs of any developing FQHSs which may be present at intermediate temperatures, but may not survive to the lowest accessible temperatures.

As seen in Fig. 3.2, our trace at $T = 6.9$ mK in the vicinity of $\nu = 2 + 3/5$ is similar to that seen in Refs. [79–81, 91, 93, 94, 96, 97], as $\nu = 2 + 3/5$ falls near bubble phase $R2b$. In the $T = 59$ mK trace of Fig.2, there is however, a slight curvature at $\nu = 2 + 3/5$. In order to establish whether this feature develops into a FQHS as the temperature is lowered, in Fig. 3.3 we examine data at intermediate temperatures. At a lower temperature at $T = 50$ mK, a resistance peak appears near $B = 4.82$ T. This peak was associated with the bubble phase and can be thought of as the precursor of the bubble phase labeled $R2c$. As the temperature is lowered to $T = 46$ mK, this peak grows and eventually splits into two at $T = 36$ mK giving way to a pronounced resistance minimum between them. Inspecting the data shown in Fig.3 we see that the precursor peaks of the bubble phase at $T = 46$ and 50 mK have a concave curvature on both sides, including one near $\nu = 2 + 3/5$. These concave features, however, cannot be associated with a developing FQHS. We thus conclude that, in spite of a fully developed FQHS at $\nu = 2 + 2/5$, in our sample we do not observe any signs of fractional correlations at $\nu = 2 + 3/5$. Recent theory work has significantly strengthened the case for a Read-Rezayi state at $\nu = 2 + 2/5$ [106–108] and has addressed the experimentally asymmetry between the observation of $\nu = 2 + 2/5$ and the missing $2 + 3/5$. Two causes for the suppression of fractional correlations at

$\nu = 2 + 3/5$ were identified: an enhanced Landau level mixing [108] and an extremely close energetic competition between the Read-Rezayi state and the bubble phase [107]. While in experiments both effects are likely to be present, results of Ref. [107] are particularly relevant for our observations.

It is to be noted that different physics may be at play at $\nu = 2 + 2/5$ and $2 + 3/5$ in GaAs/AlGaAs electron gases with two electric subbands occupied, such as electron gases confined to wide quantum wells. In contrast to samples with a single subband
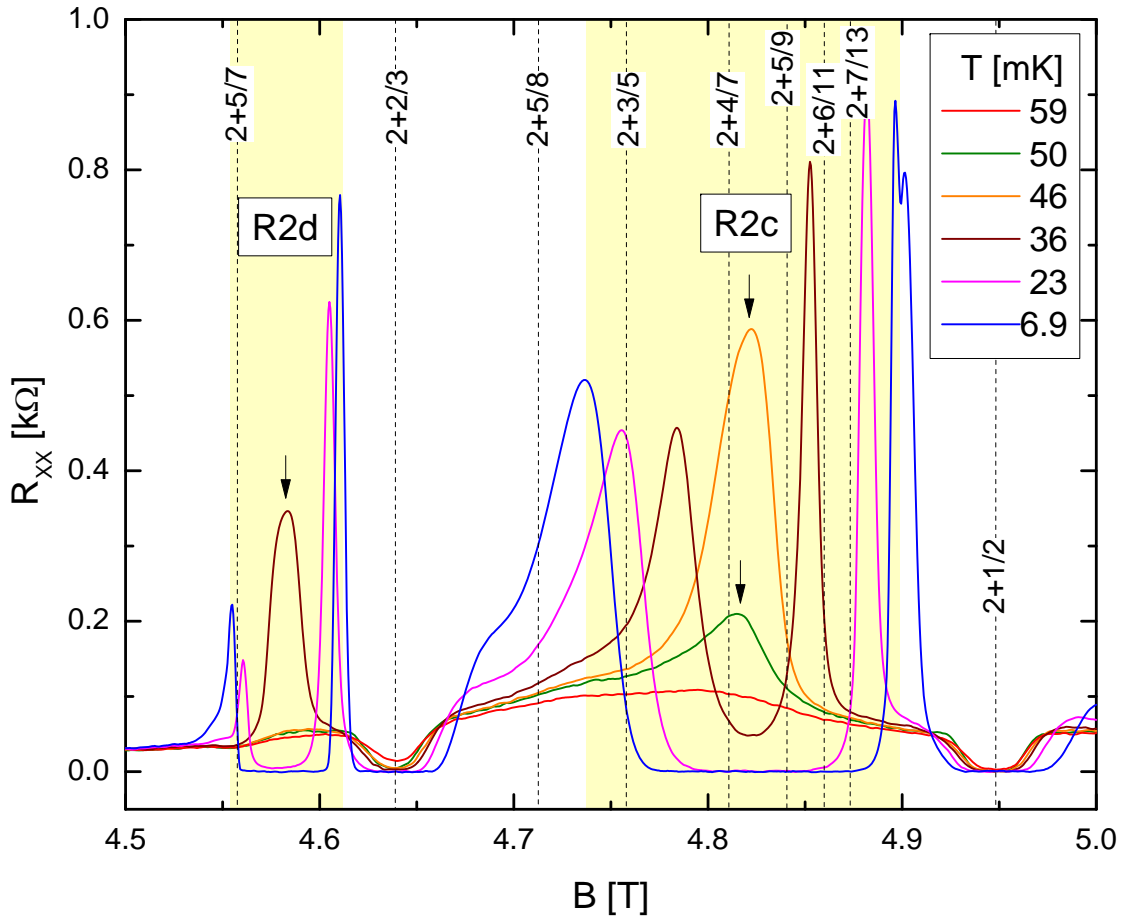
Figure 3.3. Details of the T-dependence of the magnetoresistance at filling factors less than $2 + 1/2$. Vertical arrows mark the precursors of the bubble phases $R2c$ and $R2d$. Reprinted figure with permission from V. Shingla et al., Phys. Rev. B **97**, 241105(R) (2018). Copyright 2018 by the American Physical Society.

populated, it was shown that in these systems, the $\nu = 2+2/5$ and $2+3/5$ filling factors can be achieved while the chemical potential is in the lowest Landau level [109, 110]. Under such circumstances, FQHSs have been observed both at $\nu = 2+2/5$ and $2+3/5$. These FQHSs, however, inherit the Laughlin-Jain correlations of the $\nu = 2/5$ and $3/5$ FQHSs commonly observed in the lowest Landau level. Furthermore, under such conditions, no bubble phases were observed, therefore no such competition between FQHSs and bubble phases takes place [109, 110].

3.3   Incipient fractional quantum Hall states at 2+2/7

In this section, we examine the filling factor range from $\nu = 2 + 1/2$ to $2 + 2/5$. There are several references that report either a bubble phase [78–80,88,91,96,97,111] or a precursor to the bubble phase in this region [98,112]. The bubble phase is labeled $R2b$ in Fig. 3.4. Signatures of fractional correlations in this region were reported only in a few experiments. A FQHS was reported at $\nu = 2 + 6/13$ in Ref. [80]; this state has since been seen in other high mobility samples [91, 94, 133]. In these experiments no other FQHSs were observed in the $2 + 2/5 < \nu < 2 + 1/2$ region [80, 91, 94, 133]. In contrast, local minima were reported at $\nu = 2+3/7$ and $2+4/9$, but the bubble phase $R2b$ was not observed in Ref. [95]. In addition, in Ref. [99], a local minimum in R_{xx} was also observed at $\nu = 2 + 4/9$, although the Hall resistance at this filling factor was not quantized. In our sample we observe a developing FQHS at $\nu = 2 + 6/13$. Furthermore, at $T = 36, 40, 46$ mK in our data, we observe precursor peaks associated with the bubble phase $R2b$. These precursor peaks exhibit a concave curvature on both of their sides, near $\nu = 2 + 4/9$ and $2 + 3/7$. However, the concave features in our sample in the vicinity of these two filling factors cannot be associated with a developing FQHS. We thus conclude, that in our sample, there is no evidence of FQHSs at $\nu = 2 + 3/7, 2 + 4/9, 2 + 5/11$ at any of the temperatures examined. From Fig. 3.3, a similar conclusion can be drawn for filling factors $\nu = 2 + 7/13, 2 + 6/11,$
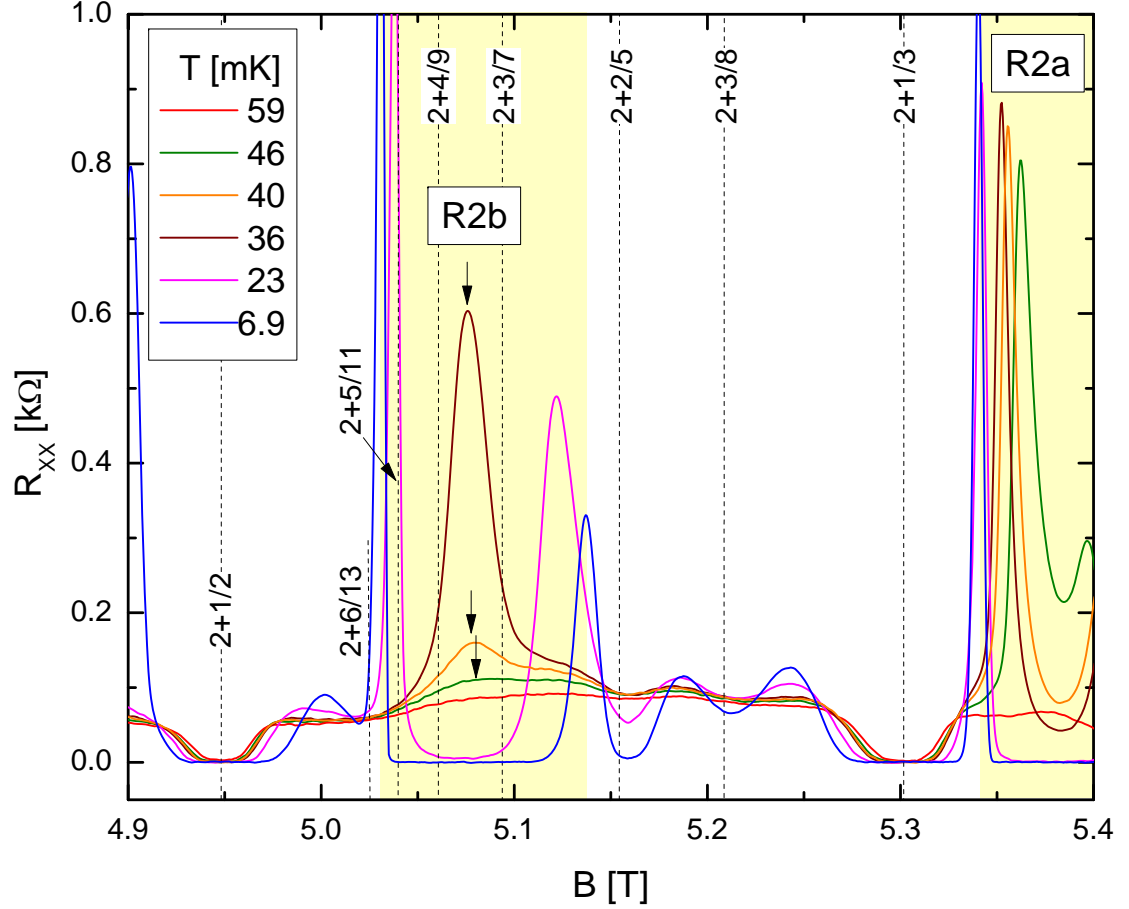
Figure 3.4. Details of the T-dependence of the magnetoresistance at filling factors larger than $2 + 1/2$. Vertical arrows mark the precursors of the bubble phases $R2a$ and $R2b$. Reprinted figure with permission from V. Shingla et al., Phys. Rev. B 97, 241105(R) (2018). Copyright 2018 by the American Physical Society.

$2 + 5/9$, $2 + 4/7$, $2 + 3/5$, and $2 + 5/8$; of these filling factors a local minimum in R_{xx} was seen at $\nu = 2 + 5/9$ in Refs. [95, 99] and at $\nu = 2 + 5/8$ in Ref. [133].

We thus found that curvatures in the magnetoresistance of our sample at the filling factors enumerated above cannot be associated with incipient fractional quantum Hall states; instead they originate from magnetoresistive fingerprints of the electronic bubble phases. In contrast to the behavior of the magnetoresistance at the filling factors discussed above, the temperature evolution at $\nu = 2 + 2/7$ is quite different.
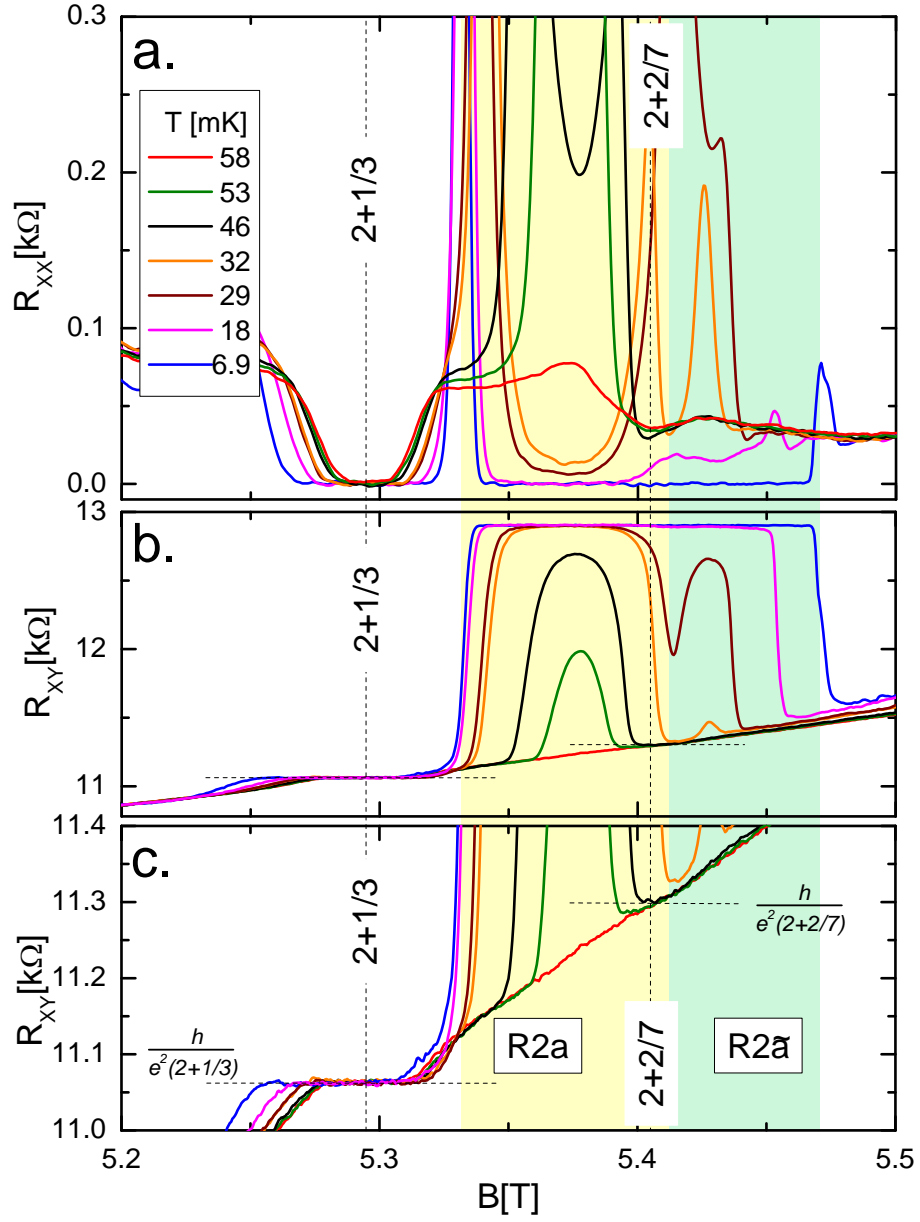
Figure 3.5. Temperature dependence of the magnetoresistance in the vicinity of $\nu = 2+2/7$ (panel a). The Hall resistance for the same range of filling factors (panel b) and a magnified view of the Hall resistance (panel c). Shading marks the bubble phases $R2a$ and $R2\tilde{a}$ at 6.9 mK. These bubble phases are separated by a deep minimum in R_{xy} seen at $T = 29$ and 32 mK, as shown in panel b. Quantization of the Hall resistance at $\nu = 2+1/3$ and at $2+2/7$ is marked by horizontal dotted lines. Reprinted figure with permission from V. Shingla et al., Phys. Rev. B 97, 241105(R) (2018). Copyright 2018 by the American Physical Society.

As discussed in Ref. [79], with the lowering of temperature, R_{xx} at this filling factor decreases and R_{xy} approaches full quantization. Our sample shows a similar behavior. Fig. 3.5a shows that at $T = 46$ mK, R_{xx} at $\nu = 2 + 2/7$ reaches its lowest value. As shown in both Fig. 3.5b and Fig. 3.5c, at this temperature and filling, R_{xy} becomes equal to $h/(2 + 2/7)e^2$ within our measurement error. In contrast to Refs. [79, 95, 98, 133], transport at the lowest temperature in our sample at $\nu = 2 + 2/7$ exhibits a fully developed reentrant insulator, i.e. $R_{xx} = 0$ and $R_{xy} = h/2e^2$. As reported earlier, near $\nu = 2 + 2/7$ there are two distinct bubble phases [79, 88], labeled $R2a$ and $R2\tilde{a}$ in Fig. 3.5. Shading in this figure denotes the stability range of these bubble phases at 6.9 mK; the two different bubbles are delimited by the deep minimum in R_{xy} shown in Fig. 3.5b. It is interesting to note that this deep minimum in R_{xy} is close to, but not at $\nu = 2 + 2/7$. We find a similar behavior at the related filling factor $\nu = 2 + 5/7$. Indeed, in Fig. 3.2 we observe a conspicuous minimum in R_{xx} at $T = 59$ mK at this filling factor. Such a local minimum was also observed in Ref. [99] and it may indicate developing fractional correlations. However, as shown in Fig. 3.3, this minimum at $\nu = 2 + 5/7$ disappears with the lowering of the temperature and the $R2d$ bubble phase prevails.

Our observations are expected to be relevant for the two-dimensional electron gas confined to bilayer graphene. Improvements in the quality of this system revealed an increasing number of FQHSs, including even denominator FQHSs [82, 83]. Details, such as the nature of the wavefunction in the $N = 1$ Landau level and the presence of the valley degree of freedom in bilayer graphene, result in differences in the physics, when compared to that in the GaAs/AlGaAs system [82,83]. Nonetheless, in addition to FQHSs, the most recent measurements in bilayer graphene also reveal reentrant integer quantum Hall effect commonly associated with bubble phases [103]. Bilayer graphene is thus expected to similar display of phase competition between FQHSs and bubble phases similar as seen in the GaAs/AlGaAs system.

3.4 Conclusion

To conclude, the development of precursors of the electronic bubble phases in the second Landau level of two-dimensional electron gases confers strong concave features to the magnetoresistance. While in our sample we find peculiar features in the magnetoresistance in the vicinity of the filling factors of interest $\nu = 2 + 3/5, 2 + 3/7, 2 + 4/9, 2 + 5/9$, and $2 + 5/8$, we cannot associate FQHSs with these filling factors neither at the lowest nor at any finite higher temperatures. We show that these features arise from the development of the magnetoresistive fingerprints of the bubble phases. In contrast, at $\nu = 2 + 2/7$ and $2 + 5/7$, we observe incipient FQHSs at intermediate temperatures, which yield to a bubble phase as the temperature is lowered further. Such a study is timely, because of the conflicting results reported in the second Landau level of the GaAs/AlGaAs system. Furthermore, our work is expected to be relevant for studies of bilayer graphene, in which an increasing number of FQHSs [82,83] as well as of bubble phases have been recently reported [103].

4. OBSERVATION OF A NOVEL CRYSTAL OF QUASILHOLES IN THE LOWEST LANDAU LEVEL

As discussed earlier, in the lowest Landau level, there is a transition from the fractional quantum Hall states to a Wigner Crystal (WC) at extremely low filling factors ($\nu <$ 1/5) [138]. In this chapter, I discuss our recent results on the observation of a related electron solid in the N=0 Landau level near higher filling factor $2-1/5$ in an extremely high mobility sample. Reentrance in Hall resistance to the nearest $\nu = 2$ plateau is observed. The partial electron filling at which such a reentrant state is observed makes a strong case for similarity to a Wigner Crystal of the quasiholes pinned by residual disorder. Our results in a narrow quantum well in an extremely low disorder sample indicate that WCs occur more often than previously thought and hint at an intricate competition of Wigner crystals and fractional quantum Hall states.

4.1   Reentrant Integer Quantum Hall State in the Lowest Landau level

The signature of reentrance observed in our data while uncommon in the N=0 Landau level, is evidence for an important set of ground states in higher Landau levels such as N=1. In addition to the FQHs and exotic even and odd denominator states such as 2+1/2 and 2+6/13 [80, 81, 91, 93, 94, 133], there is numerous reentrant integer quantum Hall states (RIQHS) [75, 76] that form. Density matrix renormalization [136] and Hartree-Fock calculations [137] predict these states to be similar to WC of electrons but with possibly one or more electrons localized at each node in the crystal. Such "bubble" phases are predicted to form only in higher Landau levels (N≥1) [40]. Therefore, similar signature of localization in the N=0 level sheds light on the importance of well-width and disorder driven phase formation of such WC like solids.

We show evidence for a reentrant state in an ultra clean 2DEGs in GaAs/AlGaAs quantum well in the upper spin branch of the N=0 Landau level. It is is seen near $\nu = 2-1/5$ manifested by a $\nu = 2$ reentrant integer quantum Hall state where the Hall resistance returns to the nearest integer value of $h/2e^2$ (where h is Planck's constant and e is the electron charge) and the longitudinal resistance R_{xx} nearly vanishes at the lowest temperatures. The quasiholes in the partially filled Landau level appear to be pinned and do not participate in conduction leading to a $\nu = 2$ plateau in Hall resistance. This report of a reentrant state in the upper spin branch in addition to the few reports at lower filling factors points to the generality of such insulating phases in the N=0 LL which were previously not expected. The partial filling factor of holes in an otherwise filled Landau level makes a strong case for resemblance to a Wigner Crystal rather than a charge density ordered phase.

Magnetotransport measurements were performed on the high quality GaAs/AlGaAs modulation doped 30nm quantum well Sample 1. The sample is 5 mm $\times$ 5 mm square with eight indium contacts diffused symmetrically on the perimeter. Previously, fragile FQHS at $\nu = 2 + 6/13$ and $3 + 1/3$ have been reported [81] in the same sample, attesting to the high quality of this sample. The He^3 immersion cell [105] which was used for the previous cooldown of this sample was rendered unsuable by a leak. In order to keep the measurements going, we opted for mounting the sample on a copper tail (shown in Figure 2.6). While this choice allowed us to continue our experiments, the same ultra-low electron temperatures could no longer be achieved. Based on available data, we estimate the lowest electronic temperature in this setup is about 12mK. A calibrated Speer thermometer was mounted on the mixing chamber for temperature measurements. AC measurements at frequency of 11Hz with lock-in techniques were used to determine the transport coefficients reported here.

In Figure 4.1, we show the main finding of this study. A plot of longitudinal resistance R_{xx} and the Hall resistance R_{xy} as a function of magnetic field at 23mK in the filling factor range $2 < \nu < 5/3$. The narrow stretch of magnetic field captures states of several types. The region highlighted in yellow shows a RIQHS $R1$ with a

minima in R_{xx} and quantization in R_{xy} corresponding to $\nu = 2$. This is the first such report of a reentrant state at a much higher filling factor close to $\nu = 2 - 1/5$ with exact filling factor $\nu = 1.788$. The peak in R_{xx} separating the plateau at $\nu = 2$ from the reentrant state $R1$ is a strong function of temperature as is shown in Fig. 2. At the lowest temperature, these plateaus merge into one another. Unlike the higher Landau levels, this reentrance in R_{xy} is a weaker feature which can be missed due to any small mixing of R_{xx} and R_{xy}. Similar reentrance and isotropic nature was verified in the orthogonal direction.
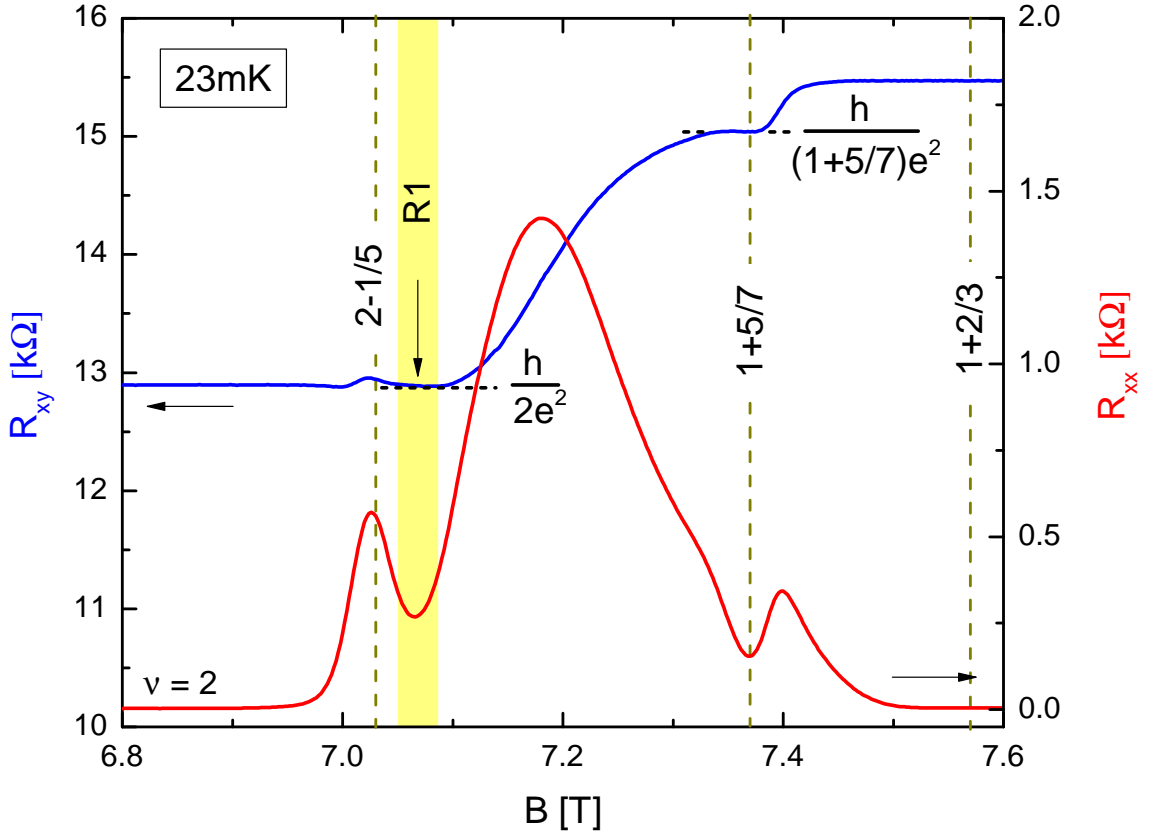
Figure 4.1. Magnetoresistance and Hall resistance plots in the upper spin branch of the lowest Landau level ($2 < \nu < 5/3$). The shaded area marks the reentrant state while the fillling factors for the other states is marked. Quantization in R_{xy} is marked with a dashed line.

In addition, a very well developed fractional state at $\nu = 1 + 2/3$ is observed which is related to the 1/3 state by particle-hole symmetry. This state form part of the Jain sequence with two quantized vortices attached to each electron and therefore is denoted as ^{2}CF state. To the left at a lower field, we report observation of a fractional state at filling factor $\nu = 1 + 5/7$. Minima in R_{xx} is accompanied by a quantization in Hall resistance at $h/(1 + 5/7)e^2$. Despite several reports on the observation of the 5/7 state [119, 120] in the lower spin branch, there has been no reports of a FQHs at this particular filling factor. Slight indications of a very weak minima in R_{xx} at this filling factor were seen in [102] but no Hall resistance data was available. The ground state at filling factor $\nu = 5/7$ has been under experimental and theoretical analysis [124–126]. Observation of a spin transition [120, 129] indicate that such a state is comprised of interacting composite fermions. However, the wavefunction written in terms of one filled Λ level of flux-four ^{4}CF is equivalent as well [124, 125]. There is however no reports near the symmetric state at 1+5/7 which could either be a symmetric state of the CF sequence $1 - p/(4p+1)$ of four-flux per electron or similar to the 5/7 comprising of interacting CFs. Our data is not sufficient to comment on the underlying particles forming this incompressible state.

4.2   Finite temperature studies in the upper spin branch of the lowest Landau level

In Figure 4.2, we show the temperature evolution of the reentrant state and the FQHS at 1+5/7 up to 75mK. As seen in the figure, the first features of the reentrant state begin to develop in R_{xx} with a splitting of a peak as seen in the trace at 75mK. Clear return of R_{xy} towards the $\nu = 2$ plateau is evident at this temperature. On further lowering the temperature to 56mK, a well minima in R_{xx} begins to develop. This evolution is similar to those of the reentrant states in the second and higher Landau levels [88, 91] indicating a collective localization. As the lowest temperature of 12mK, the magnetoresistance nearly vanishes. Concomitantly, the Hall resistance approaches
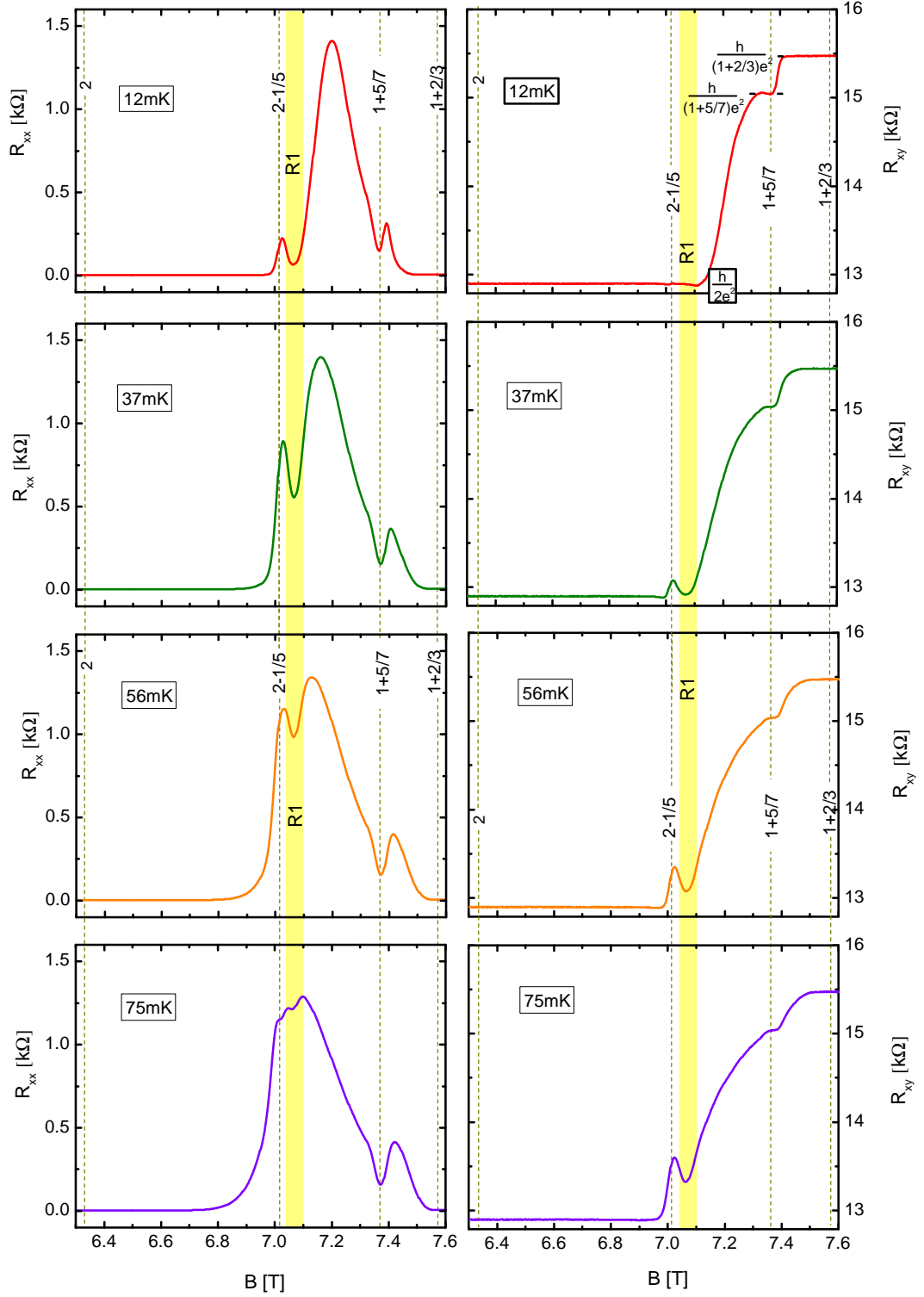
Figure 4.2. Temperature evolution of the longitudinal and Hall resistance is shown up to 75mK in the filling factor range $2 < \nu < 5/3$. Filling factors of interest are marked. At the lowest temperature of 12mK, the reentrant integer state is fully developed.

$h/2e^2$, corresponding to the nearest integer value. However, at this temperature, the plateau at the $\nu = 2$ integer state and the reentrant state merge.

On the other hand, the state at $\nu = 1+5/7$ shows peculiar temperature dependence as seen in the figure. The longitudinal resistance at this filling is indifferent to changes in temperatures up to 75mK with both R_{xx} and R_{xy} showing features of a well-developed FQHs. Contrary to the activated behavior of a FQHS given by $R_{xx} \propto \exp(-\Delta/2k_B T)$, the gap at filling factor $\nu = 1+5/7$ is not activated for temperatures upto 75mK. With a clear minimum in R_{xx} and a robust quantization in R_{xy}, this non-activated behavior of the gap is very puzzling. This behavior cannot be associated with lack of electron cooling as the plateau width at $\nu = 1 + 2/3$ clearly increases with lower temperatures in addition to the strong temperature dependence at adjacent RIQHS shown in Figure 4.2, both serving as strong evidence for the lower electron temperatures. The weakly developed FQHS at this filling factor likely is a consequence of phase competition with the nearby electron solid at R1.

It is useful to examine the temperature evolution at the exact filling factor of the RIQHS and compare it to the temperature evolution in both R_{xx} to those of the RIQHS in the second Landau level [88] to predict the nature of the solid formed leading to the reentrant behavior. In Figure 4.3, we show evolution with temperature of the minima in longitudinal resistance R_{xx} and Hall resistance R_{xy} as a function of temperature. A peak in R_{xx} at a temperature of about a 100mK is similar to those of the reentrant states in the higher Landau levels such as the N=1 [88,91]. The peak at $R1$ is much broader in comparison and falls off slowly as a function of temperature. In the higher Landau levels, this peak is associated with the signature of collective localization [88]. The Hall resistance on the other hand undergoes a transition from the nearest integer quantized value to the classical Hall resistance $h/\nu e^2$ which is marked in the figure. We note that the Hall resistance almost approaches this value within 60Ω. Both the evolution of R_{xx} and R_{xy} at $R1$ is qualitatively similar to those of the reentrant states in the higher Landau levels. The reentrant states in the higher Landau levels are understood as electron solids called bubble phases. However, in

the N=0 Landau Level, such bubble phases are not expected [40–43]. Therefore, we suggest the collective localization features to be indicative of a formation of a Wigner crystal of electrons.
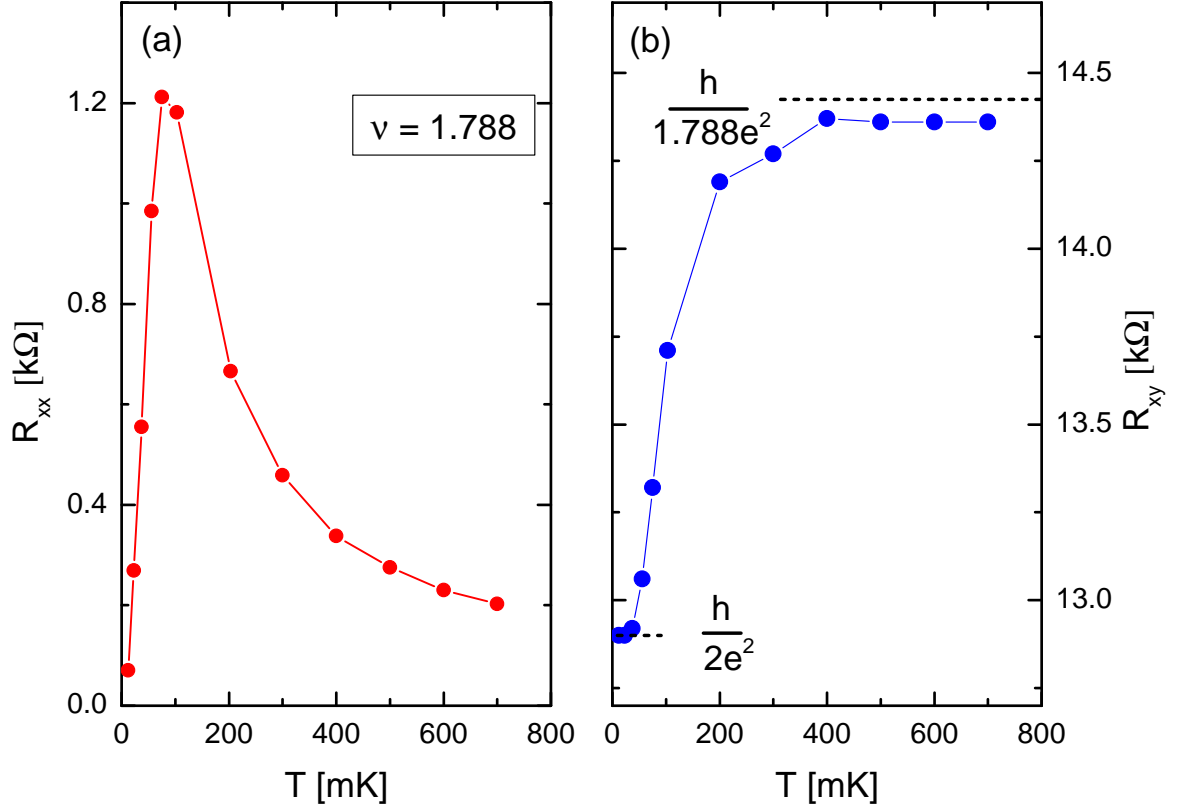
Figure 4.3. (a) Temperature dependence of the minima in R_{xx} at filling factor $\nu = 1.79$ for temperatures upto 700mK. The peak observed near 100mK may indicate the first correlations of a solid phase. (b) The evolution of R_{xy} at the RIQHS (Reentrant Integer Quantum Hall State) from the quantized value at $h/2e^2$ almost reaching the classical value at the highest temperatures.

4.3 Density effects

As a further test of the $R1$ phase, we studied its evolution as a function of changing electron density. We employed the technique used previously [139] of low temperature illumination where a red LED was used with low currents ($\sim 1\mu A$) at milliKelvin

temperatures to decrease the sample density. In Figure 4.4, such a evolution with decreasing density is shown. As the density is decreased to $2.88 \times 10^{11} \mathrm{cm}^{-2}$, the quantization features of this reentrant state begin to weaken and eventually wash out with lowering the density further. In contrast to an earlier study near $4/5$ [128] where the fractional state at $4/5$ is appears and disappears with changing density, we do not see any quantization at the nearby filling factor $2 - 1/5$ in the range of electron densities that were accessible. The mobility of the sample decreased by about a factor of three from the highest in grown density to the lowest density of $2.6 \times 10^{11} \mathrm{cm}^{-2}$. Observations of the RIQHS labeled R1 at the sample filling factor over a range of densities reinforce the association of this transport feature with a genuine ground state, identified earlier as the WC.
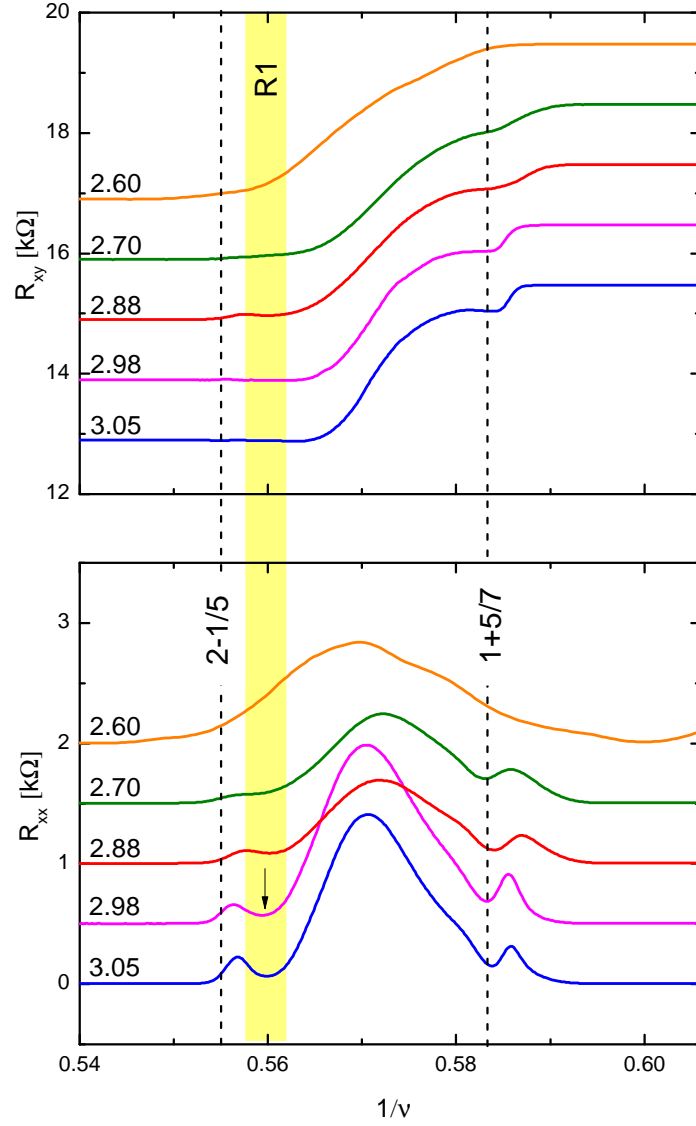
Figure 4.4. Waterfall plot of the magnetoresistance and Hall resistance plots as function of changing sample density plotted vs $1/\nu$ with densities indicated in units of 10^{11} cm^{-2}. The reentrant state $R1$ disappears as the density is decreased to 2.88×10^{11} cm^{-2} using low temperature sample illumination.

4.4   Discussion

For comparison with earlier reports of such insulating phases at lower filling factors, we compute the partial filling factors. For electrons in the filling factor range 2

$< \nu < 1$, $\nu = 2 \pm \nu^*$ can be considered as two filled inert LLs plus excess electrons or holes with filling factor ν^* which may conduct. In our case near at $\nu = 1.79$, the excess particles is holes and therefore form a solid which does not contribute to conduction, namely a solid of quasiholes.

There is a study which reports such reentrant states [127] between 2/3 and 3/5 and its particle-hole conjugate state in between 1/3 and 2/5 for electrons which resides in QW wells made with $Al_xGa_{1-x}As$ alloy. They interpret their insulating states as pinned WC states due to the short-range (alloy) disorder. That interpretation does not seem to explain the reentrant state we observe in an ultra-clean sample with a much lower disorder. On the other hand, high frequency resonances have been reported [115] near ν=1 and 2 indicating insulating behavior. These microwave resonance has been interpreted as collective pinning of a Wigner Crystal phase. However, the partial electron filling factors for such features is $\nu^* < 0.15$ which is smaller than the $\nu^* = 0.21$ at which we observe the insulating phase.

The RIQHS we observe is at $\nu^* \simeq 0.21$ is remarkably close to one of the insulating phases observed by Liu et. al [128] at $\nu^* \simeq 0.22$. This observation near $\nu = 1 \pm 1/5$ in a wide QW system which appears above a critical electron density n_c is understood as the large electron layer thickness inducing a WC formation. In their sample, the QW width is several times the magnetic length given by W/l_B which ranges from 4.6 to 6.0 for their critical density. In our sample, where we observed the RIQHS at a fixed electron density in a 30nm well, the W/l_B is ~ 3.1 which is much lower in comparison. However, the mobility of our sample is about 5 times higher making the disorder potential very different and a direct comparison difficult. Also, we could not access the region near $\nu = 1$ in our sample due to the limitation on the magnetic field available. The same group published another study [129] in which the insulating phase near 4/5 is interpreted as a ^{2}CF ferromagnetic crystal in a 65nm wide sample. Such wide quantum well samples are often populated in the second electric subband making the physics very different from single subband occupation [131]. The nature of the electron wavefunction may play a significant role in the transition between

different spin states that they report. We do not see any such transitions when the density was lowered by more than 10% as seen in Figure 4.4.

To compare these reentrant states to the bubble phases observed in the higher Landau levels, we compare the central filling factors ν^* to that of $R1$. From ref. 32, the partial filling factors for the 8 states in N=1 and 4 reentrant states in N=2, $\nu^* > 0.288$ which is much larger than the the partial filling factor for the reentrant state in the LLL of 0.21. This, however is quite close to the filling factor near $\nu = 1/5$ at which a WC has been observed. Therefore, there is conclusive evidence for the renetrant state in the LLL to be a Wigner Crystal. Our interpretation is in agreement with prior reports of such insulating phases seen elsewhere in the lowest Landau level [127, 128].

4.5 Conclusion

We have reported an observation of a reentrant integer quantum Hall state at a high filling factor of 1.788 in an ultra high mobility GaAs/AlGaAs 30nm quantum well. The temperature dependence of such a state in the lowest Landau level points to a collective pinning mechanism of quasiholes forming a Wigner Crystal based on the partial filling factor of electrons. Observation of yet more insulating phases in the N=0 Landau level and new fractional states even after several decades points to the rich electron physics that may continue to surface with improvements in sample quality.

5. OBSERVATION OF AN EXOTIC SOLID OF COMPOSITE FERMIONS

The recent proliferation of two-dimensional materials has lead to renewed interest in interactions driven emergent phenomena. Such interactions between fundamental particles can drive the system to have non-trivial topological order in some cases. In this chapter, we discuss a novel effect of interaction-driven quasiparticles (Composite Fermions) forming charge density waves in the vicinity of $\nu = 1 + 2/3$ fractional quantum Hall state (FQHE) in an extremely high quality two-dimensional electron system (2DES) in GaAs/AlGaAs quantum well. A minima is R_{xx} is accompanied by quantization in R_{xy} at $3h/5e^2$ in the N=0 Landau level indicates that a exotic electron solid of composite fermion quasiparticles is involved. This is the first such observation of a reentrant fractional quantum Hall effect in transport measurements.

Interactions between fundamental particles in condensed matter systems play an essential role in determining a variety of phases that form. Such strongly interacting particles reorganize themselves to form new weakly interacting particles such as Cooper pairs in superconductors, magnons in a magnet and phonons in a lattice as few examples. Theoretically, one can then solve the problem in terms of these weakly interacting quasiparticles. In the case of a two-dimensional electron gas, as a result of strong Coulomb interactions between these electrons, composite fermions (CFs) [5] emerge as the weakly interacting quasiparticles. In all such systems, one always wonders if these collective many-body entities have a real existence in the system or are just a theoretical concept. It is of no doubt that such particles cannot exist in isolation but may behave similarly to isolated particles in the interacting environment.

5.1 Interacting Composite Fermions

One important aspect of these emergent quasiparticles is the nature of interactions between them. In the simplest approximation, the interactions can be ignored and an important class of ground states such as most of the odd-denominator FQHS in the N=0 Landau level can be explained with this simple assumption. However, under certain limits, just like electrons, these residual interactions between these CFs become significant and cannot be ignored. Some such examples include the CF pairing at the even denominator $\nu = 5/2$ FQHS state [23, 77]. There has been a growing number of reports in other materials such as graphene [134] and ZnO [135] where such inter-CF interactions have lead to consequential experimental results.

5.2 Reentrant Fractional Quantum Hall Effect

Sample 1 used for this study is a high quality GaAs/AlGaAs modulation doped 30nm quantum well grown by molecular beam epitaxy. The setup as described in Chapter 2 with a copper mount was used in this study. Low temperature illumination of the sample at 10K with a red LED preceded prior to transport measurements. AC measurements were performed at frequency of 11Hz with lock-in techniques to determine the transport coefficients reported here.

In Fig. 5.1, we show the Hall resistance R_{xy} and the magnetoresistance R_{xx} trace in the upper spin branch of the N=0 Landau level plotted as a function of magnetic field B at T=12mK. Well quantized odd-denominator fractional quantum Hall states on both sides of filling factor 1+1/2 are marked. The high quality of the sample is evidenced by the deep minima in R_{xx} and well quantized plateaus in R_{xy} at many Jain sequence states with two quantized vortices attached given by the symmetric states of the sequence $1/2p \pm 1$, where p is an integer. Robust FQHS at filling factors 1+2/3, 1+3/5, 1+4/7, 1+5/9, 1+6/11, 1+5/11, 1+4/9, 1+3/7, 1+ 2/5 and 1+1/3 with minima in R_{xx} and well developed plateau in R_{xy} are observed. At the higher magnetic fields, two symmetric FQHS of the higher CF sequence $1/4p \pm 1$ at $1 + 2/7$
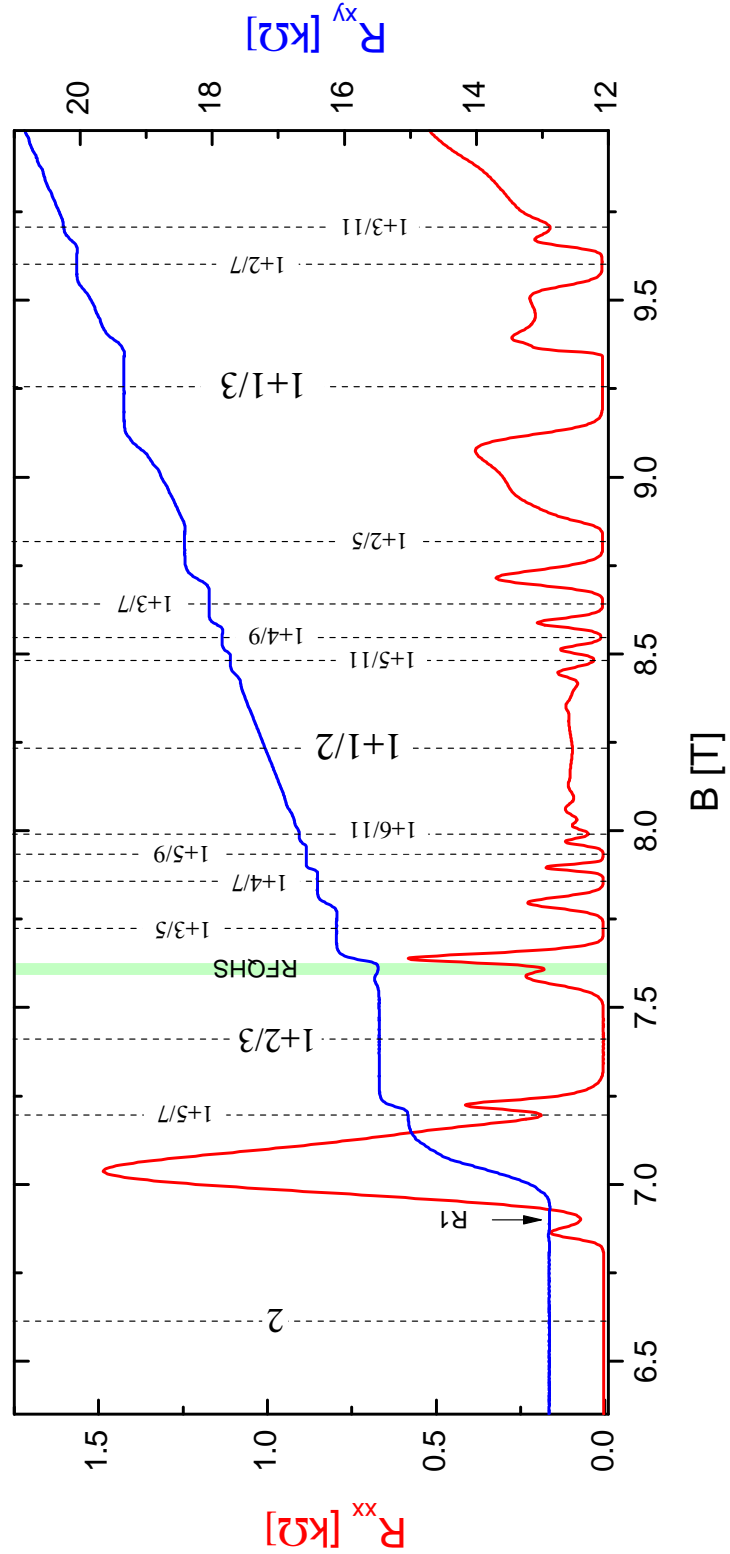
Figure 5.1. Magnetoresistance R_{xx} and Hall resistance R_{xy} at 12mK as a function of magnetic field B. Filling factors mark the fractional and integer quantum Hall states as well as some filling factors of importance. The RIQHS (Reentrant Integer Quantum Hall State) is marked while the RFQHS (Reentrant Fractional Quantum Hall State) is shown with green shading.

and $1 + 3/11$ are observed. Observations of many FQHS warrants to the high quality of the sample. The most interesting feature of this trace is highlighted in green which shows a minima in R_{xx} accompanied by a quantization in Hall resistance to the nearest fractional value of the $1+2/3$ state.

To study this feature, we focus on this region in Fig. 5.2. The intriguing feature at a slightly higher field from the $1+2/3$ FQHS shows a minima in R_{xx} and a reentrance in R_{xy} to the *value of the adjacent fractional quantum Hall state corresponding to* $h/(1+2/3)e^2$. This observation is in contrast to the Reentrant Integer Quantum Hall
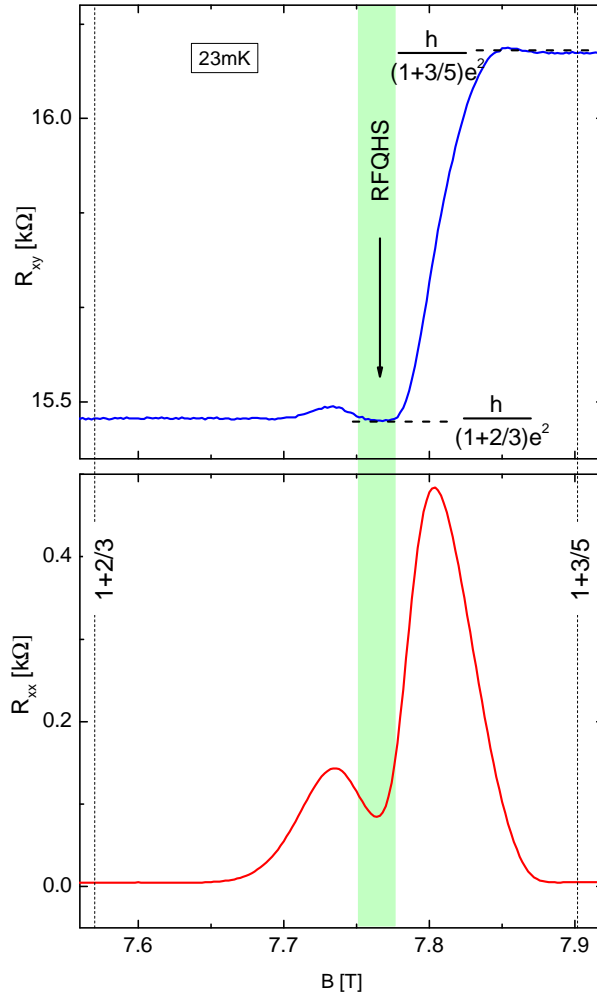
Figure 5.2. Magnified magnetoresitance and Hall trace at 23mK showing the reentrant fractional state highlighted in green.

states (RIQHE) where the quantization in R_{xy} is to the nearest integer value. We therefore, term it as the Reentrant Fractional Quantum Hall Effect (RFQHE). This is the first such observation of this effect. Since R_{xy} is quantized to a fractional value, one can be sure that CF quasiparticles are involved in the formation of this electron solid. Specifically, flux-two CFs are involved. Hence we are dealing with a very special quantum solid, in which complex electron correlations play a fundamental role.

In order to examine the solid of CFs more closely, we will examine the filling factor at which it forms. The electron filling factor at which this new phase RFQHS is observed is $\nu = 1.63$. The corresponding filling CF filling factor [14] is 1.42. This filling factor can then be considered as one filled Λ level of composite fermions and one partially filled level $\nu^* = \nu_f + \nu_p = 1 + 0.42$. The partial CF filling factor ν_p is very close to those of the electron bubble phases observed in the higher (N≥1) Landau levels [91]. This bubble phase of CFs is nestled between two FQHS liquid states comprising of ^{2}CF on the lower field and the higher field state at $\nu = 1 + 3/5$ state. A transition to a solid like phase occurs between the two liquid phases.

As a further test for the new reentrant phase, we studied sample 2 which is similar in density at $n = 3.0 \times 10^{11}/\text{cm}^2$ and low-temperature mobility $\mu = 2.8 \times 10^7 \text{ cm}^2/\text{Vs}$. As seen in Figure 5.3, the longitudinal resistance almost vanishes near the same filling factor. However, no Hall resistance data was collected for this sample at the lowest temperature of 12mK. The vanishing of R_{xx} at a very similar filling factor is extremely convincing of a universal phenomena at play in extremely high quality samples.
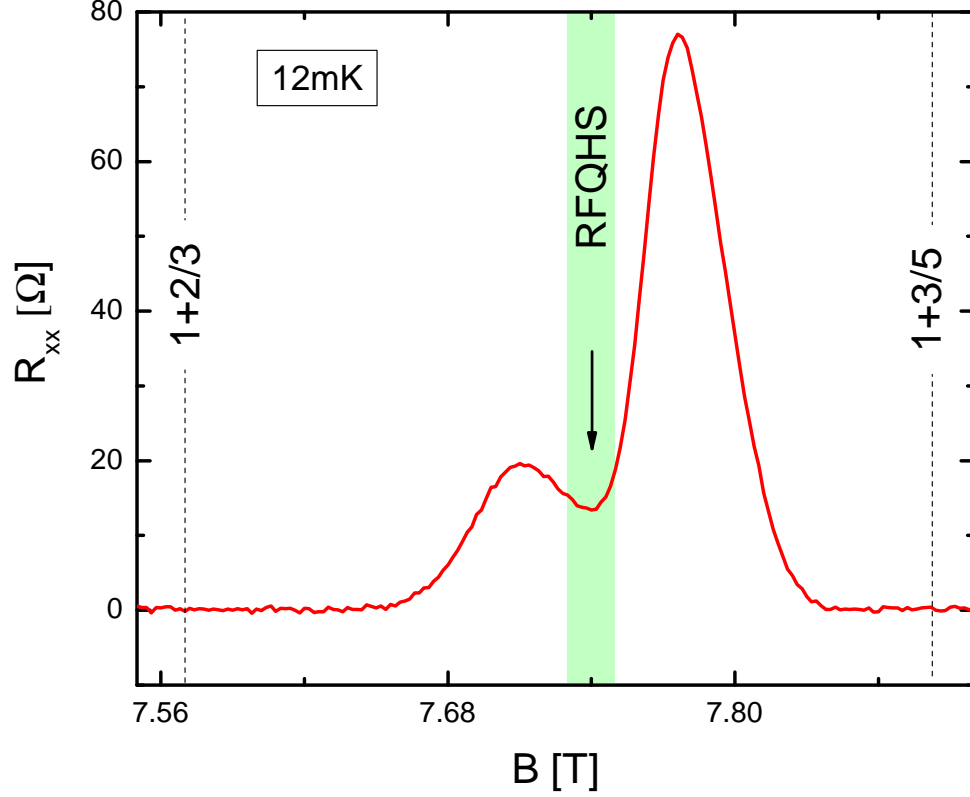
Figure 5.3. The magnetoresistance trace in sample 2 where the RFQHS (Reentrant Fractional Quantum Hall State) is observed as well. The sample parameters are very similar to the one shown in the main text. The same appearance of RFQHS in another sample lends support to the universality of this phenomena which may be extremely sensitive to the disorder potential.

5.3 Temperature dependence of the reentrant fractional quantum Hall effect

To further investigate such reentrance in the lowest Landau level, we look at the detailed temperature dependence in Figure 5.4. At the highest temperature of 100mK, the Hall resistance almost has a plateau like appearance but with no quantization in R_{xx}. The first features of this exotic crystal state begin to appear close to 56mK with a slight depression in magnetoresistance. As the temperature is lowered, the Hall

resistance approaches towards the plateau of the nearest fractional state at $\nu = 1+2/3$ which a particle-hole of the 1/3 state in the other spin branch of the lowest Landau level. R_{xx} at the lowest temperature of 12mK is few tens of ohm. However, the Hall resistance at this temperature has a very small peak separating the reentrant state and the plateau at the fractional state. Unlike the electron reentrant states in the higher Landau levels, where huge peaks separate the reentrant states from the adjacent fractional states, such a peak is much weaker in the case of RFQHS. the first precursors of these ordered phases begins with a peak which eventually splits into two giving way to the plateau in R_{xx}, we do not see such behavior for this phase comprising the CFs. Due to the relatively weak CF-CF interactions as compared to the electron-electron correlations, such signatures of a CF crystal are expected to be suppressed in transport measurements [145].

5.4   Discussion

We begin with discussing some of the recent experiments which have indicated a correlated CF Wigner Crystal (CFWC) in GaAs and compare with how our present finding stands out adding another dimension to the current understanding of inter-CF interactions. The first such report was in microwave resonance experiment by Engel's group [141] where resonances near the 1/3 FQHS state in the lowest Landau level is associated with a type-II CFWC [148, 149]. The microwave signal at these fillings factors was much smaller than those observed near integer fillings and they report a drift in the data that was used to offset the resonance features. The partial CF filling factors at which such microwave frequency resonance was reported is near $\nu^* \sim \pm 0.15$ which is about a factor of three smaller than out results at $\nu^* = 0.42$. Such a stark difference in partial filling factors clearly points to CF solids of fundamentally different nature in these two experiments. A type-II CFWC is expected to form [148] at the filling factor they report where the CFs in the partially filled Λ level localize in a Wigner Crystal arrangement due to residual CF-interactions. No such results in
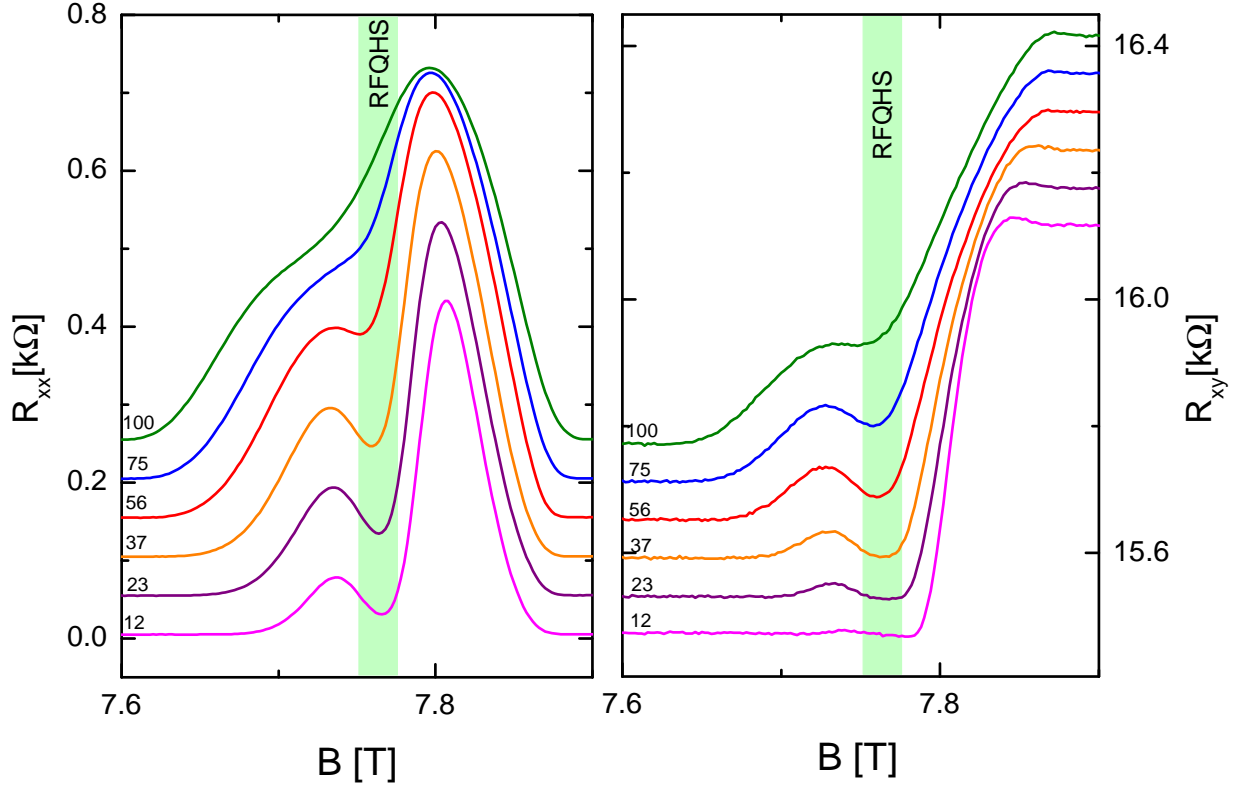
Figure 5.4. Temperature evolution in the vicinity of RFQHS (Reentrant Fractional Quantum Hall State) in R_{xx} and R_{xy} from the lowest temperature of 12mK to 100mK. The first features of the reentrant state begin to develop around 75mK.

transport near these filling factors have been reported perhaps due to the weakness of the localization. In addition, the sample under such study is a 50nm QW with a mobility of 15×10^6 cm^2/Vs. Our results in a 30nm QW have a higher confining potential with only single subband occupation (which is verified with the observation of a well quantized FQHS at $\nu = 5/2$). In addition, our mobility is higher by a factor of two making the disorder potential very different. Therefore, the filling factors and the difference in sample parameters make a compelling case for the different physics at play.

Another interesting study where a CF ferromagnetic WC is claimed [142] observe a reentrance to the nearest integer state at near fractional filling factor 4/5. A transition in the nearby FQHS state with changing density is taken to be evidence for the formation of such a CF Crystal. However, they do not see reentrance in Hall resistance to the nearest fractional value which makes our observation in line with those of charge density ordered phase of CFs similar to the electron bubble phases in the higher Landau level.

We next discuss the arguments on why our observation may be in agreement with a charge density wave of composite fermions (a cluster of particles localized). The RFQHS is observed at an electron filling factor of $\nu = 1.63$ which corresponds to a CF filling factor of $\nu^* = 2.42$. The partial CF filling factor expected from theoretical studies for a bubble phase formation is $\nu^* < 0.4$ [145] which is very close to where such reentrance is reported at $\nu^* = 0.42$. As a further evidence, this partial filling of CFs is particularly close to those of reentrant electron bubble phases in the second Landau level [75, 76, 91]. There is strong evidence of such electron reentrant states to form bubbles (more than one electron) at each lattice lattice [88, 91, 140].

A natural question of which flavor of CF (either with two or four vortices attached) comprising this novel solid phase arises. We try to understand this by looking at the region where such a state forms in the lowest Landau level. The reentrance observed is nearest to the FQHS at 1+2/3 which is a ^{2}CF state with a filling factor of 1.67. This filling factor range falls in the region of effective negative field experienced by

the composite fermions. Therefore, as we move to higher magnetic fields towards 3/2, the occupancy of the CF Λ level increases. As the magnetic field is increased, quasiparticle excitations from the last occupied $\Lambda = 1$ begin to populate the next Λ level resulting in a partially filled level at CF filling factor 1.42. The next FQHS at $\nu = 1 + 3/5$ is also a ^{2}CF state. Therefore, it is very likely for the partially filled state to comprise of ^{2}CF particles localizing as bubbles forming a triangular lattice.

There has been a very recent result discussing the effect of electron orbital wavefunction on the number of particles localized in the electron bubble formation in N=3 Landau levels [140]. It is somewhat difficult to discuss the same for composite fermions as the exact form of the wavefunctions are not known the the CF Λ levels. In Ref. 9, a *variational* wavefunction for CFs is considered for solving the problem in a partially filled Λ level in a planar geometry. They found that the inter-CF interaction is attractive in most cases making a strong case for charge density waves. Several works have concluded a stripe phase to be most favorable at half-filling of CF levels with a periodicity which is several times the magnetic length. Therefore, at a filling factor close to half-filling, it is only natural to expect a bubble phase ($M > 1$) which then translates to a broken rotational symmetry at exact half filling.

5.5 Conclusion

In conclusion, we report the first evidence of a reentrant fractional quantum Hall effect in the lowest Landau level of GaAs electron gas. Such a phase is indicative of a exotic bubble crystal of composite fermions in contrast to the charge density waves of electron crystals observed in higher Landau levels. The partial CF filling factor is very close to those of the partial electron filling factors in the second Landau level where such reentrant integer quantum Hall effect is routinely observed. Such interaction-driven composite fermion crystal is an important milestone in the current understanding of novel correlated electron solids.

REFERENCES

[1] K. von Klitzing, G. Gorda, and M. Pepper, Phys. Rev. Lett. **45**, 494 (1980).

[2] P.W. Anderson, Phys. Rev. **109**, 1492 (1958).

[3] D. Tsui, H. Stormer and A.C. Gossard, Phys. Rev. Lett. **48**, 1559 (1982).

[4] R. B. Laughlin, Phys. Rev. Lett. **50**, 1395 (1982).

[5] J.K. Jain, Phys. Rev. Lett. **63**, 199 (1989).

[6] J.P. Eisenstein and H.L. Stormer, Science **248**, 1510-1516 (1990).

[7] E. Wigner, Phys. Rev. **46**, 1002 (1934).

[8] A. Stern Nature **464**, 187-193 (2010).

[9] H.L. Störmer, D.C. Tsui, and A.C. Gossard, Rev. mod. Phys. **71**, S298 (1999).

[10] D.C. Tsui, Rev Mod. Phys. **71**, 891 (1999).

[11] B. Jeckelmann and B. Jeanneret, Séminaire Poincaré **2**, 39 (2004).

[12] M. Büttiker, Phys. Rev. B **38**, 9375 (1988).

[13] R. Landauer, IBM J. Res. Dev. **1**, 223 (1957).

[14] J.K. Jain, *Composite Fermions* (Cambridge University Press, Cambridge, England, 2007).

[15] F. Pobell *Matter and Methods at Low Temperatures* (Springer 2007).

[16] X.G. Wen, *Quantum Field Theory of Many-Body Systems* (Oxford University Press, Oxford, UK, 2004).

[17] R. Shankar *Principles of Quantum Mechanics* (Springer Science, 1994).

[18] R.E. Prange and S.M. Girvin *The Quantum Hall Effect* (Springer, 1987).

[19] J.H. Davies *The Physics of Low-Dimensional Semiconductors* (Cambridge University Press, 1998).

[20] *Perspectives in Wuantum Hall Systems* edited by S.D. Sarma and A. Pinczuk (Wiley 2004)

[21] R. Willett, J.P. Eisenstein and H.L. Stormer, D.C. Tsui, A.C. Gossard and J.H. English, Phys. Rev. Lett. **59**, 1776 (1987).

[22] F.D.M. Haldane and E.H. Rezayi, Phys. Rev. Lett **60**, 956 (1988).

[23] G. Moore and N. Read, Nucl. Phys. B **360**, 362 (1991).

[24] B.I. Halperin, P.A. Lee, and N. Reed, Phys. Rev. B **47**, 7312 (1993).

[25] R.H. Morf, Phys. Rev. Lett. **80**, 1505 (1998).

[26] S.S. Lee, S. Ryu, C. Nayak, M.P. Fisher, Phys. Rev. Lett **99**, 236807 (2007).

[27] M. Levin, B.I. Halperin, B. Rosenow, Phys. Rev. Lett. **99**, 236806 (2007).

[28] K.A. Schreiber, N. Samkharadze, G.C. Gardner, Y. Lyanda-Geller, M.J. Manfra, L.N. Pfeiffer, K.W. West, and G.A. Csáthy, Nat. Comm. **10**, 1038 (2018).

[29] W. Pan, H.L. Stormer, D. Tsui, L. Pfeiffer, K. Baldwin, K. West, Phys. Rev. Lett. **90**, 016801 (2003).

[30] W. Kang, H.L. Stormer, L.N. Pfeiffer, K.W. Baldwin, and K.W. West, Phys. Rev. Lett. **71**, 3850 (1993).

[31] R.R. Du, H.L. Stormer, D.C. Tsui, L.N. Pfeiffer and K.W. West, Solid St. Comm. **90**, 71 (1994).

[32] W. Kang, H.L. Stormer, L.N. Pfeiffer, K.W. Baldwin, K.W. West, Physics B **211**, 396 (1995).

[33] M.A. Mueed, D. Kamburov, S. Hasdemir, M. Shayegan, L.N. Pfeiffer, K.W. West, and K.W. Baldwin, Phys. Rev. Lett. **114**, 236406 (2015).

[34] R.L. Willett, M.A. Paalanen, R.R. Ruel, K.W. West, L.N. Pfeiffer, and D.J. Bishop, Phys. Rev. Lett. **54**, 112 (1990).

[35] M. Greiter, X.G. Wen, and F. Wilczek, Phys. Rev. Lett. **66**, 3205 (1991).

[36] C. Nayak, S.H. Simon, A. Stern, M. Freedman, S. Das Sarma, Rev. Mod. Phys. **80**, 1083 (2008).

[37] A.Y. Kitaev, Ann. Phys. **301**, 2-30 (2003).

[38] D. Sarma, M. Freedman, and C. Nayak, Phys. Rev. Lett. **94**, 166802 (2005).

[39] M. Freedman, A. Kitaev, M.J. Larsen, and Z. Wang, Bull. Am. Math. Soc. **40**, 31-38 (2003).

[40] A.A. Koulakov, M.M. Fogler, and B.I. Shklovskii, Phys. Rev. Lett. **76**, 499 (1996).

[41] M. M. Fogler, A. A. Koulakov, and B. I. Shklovskii, Phys. Rev. B 54, 1853 (1996).

[42] M. M. Fogler, Stripe and bubble phases in quantum Hall systems in High Magnetic Fields: Applications in Condensed Matter Physics and Spectroscopy (Springer, Berlin, 2001).

[43] R. Moessner and J.T. Chalker, Phys. Rev. B, **54**, 5006 (1996).

[44] E. Fradkin and S.A. Kivelson, Phys. Rev. B **59**, 8065 (1999).

[45] K. B. Cooper, M. P. Lilly, J. P. Eisenstein, L. N. Pfeiffer and K. W. West. Phys. Rev. B **60**, R11285 (1999).

[46] X. Wang, H. Fu, L. Du, X. Liu, P. Wang, L.N. Pfeiffer, K.W. West, R.R. Du, and X. Lin, Phys. Rev. B **91**, 115301 (2015).

[47] S. Baer, C. Rossler, S. Hennel, H.C. Overweg, T. Ihn, K. Ensslin, C. Reichl, and W. Wegscheider, Phys. Rev. B **91**, 195414 (2015).

[48] A.V. Rossokhaty, Y. Baum, J.A. Folk, J.D.Watson, G.C. Gardner, and M.J. Manfra, Phys. Rev. Lett. **117**, 166805 (2016).

[49] K. Bennaceur, C. Lupien, B. Reulet, G. Gervais, L.N. Pfeiffer, and K.W. West, Phys. Rev. Lett. **120**, 136801 (2018).

[50] B. Friess, V. Umansky, K. von Klitzing, and J.H. Smet, Phys. Rev. Lett. **120**, 137603 (2018).

[51] M.E. Msall and W. Dietsche, New J. Phys. **17**, 043042 (2015).

[52] B. Friess, Y. Peng, B. Rosenow, F. von Oppen, V. Umansky, K. von Klitzing, and J.H. Smet, Nature Phys. **13**, 1124 (2017).

[53] R.L. Willett, C. Nayak, K. Shtengel, L. N. Pfeiffer, and K. W. West, Phys. Rev. Lett. **111**, 186401 (2013).

[54] W.E. Chickering, J.P. Eisenstein, L.N. Pfeiffer, and K.W. West, Phys. Rev. B **87**, 075302 (2013).

[55] R.M. Lewis, P.D. Ye, L.W. Engel, D.C. Tsui, L.N. Pfeiffer, and K.W. West, Phys. Rev. Lett. **89**, 136804 (2002).

[56] R.M. Lewis, Y.P. Chen, L.W. Engel, D.C. Tsui, L.N. Pfeiffer, and K.W. West, Phys. Rev. B 71, 081301 (2005).

[57] G. Sambandamurthy, R. M. Lewis, H. Zhu, Y. P. Chen, L.W. Engel and D.C. Tsui, Phys. Rev. Lett. **100**, 256801 (2008).

[58] T.S. Lay, J.J. Heremans, Y.W. Suen, M.B. Santos, K. Hirakawa, M. Shayegan, and A. Zrenner, Appl. Phys. Lett. **62**, 3120 (1993).

[59] B. A. Piot, J. Kunc, M. Potemski, D. K. Maude, C. Betthausen, A. Vogl, D. Weiss, G. Karczewski, and T. Wojtowicz, Phys. Rev. B **82**, 081307 (2010).

[60] K. Lai, W. Pan, D.C. Tsui, S. Lyon, M. Mühlberger, and F. Schäffer, Phys. Rev. Lett. **93**, 156805 (2004).

[61] Q. Shi, M.A. Zudov, C. Morrison, and M. Myronov, Phys. Rev. B **91**, 241303 (2015).

[62] O.A. Mironov, N. d'Ambrumenil, A. Dobbie, D.R. Leadley, A.V. Suslov, and E. Green, Phys. Rev. Lett. **116**, 176802 (2016).

[63] J. Falson and M. Kawasaki, Rep. Prog. Phys. **81**, 056501 (2018).

[64] T.M. Kott, B. Hu, S.H. Brown, and B.E. Kane, Valley-Degenerate Two-Dimensional, Phys. Rev. B **89**, 041107 (2014).

[65] A.K. Geim and K.S. Novoselov, Nature Materials **6**, 183 (2007).

[66] S. Manzeli, D. Ovchinnikov, D. Pasquier, O.V. Yazyev, and Andras Kis, Mature Reviews Materials **2**, 1 (2017).

[67] F. Yang, Z. Zhang, N.Z.Wang, G.J. Ye, W. Lou, X. Zhou, K.Watanabe, T. Taniguchi, K. Chang, X.H. Chen, and Y. Zhang, Nano Lett. **18**, 6611 (2018).

[68] K. I. Bolotin, F. Ghahari, M. D. Shulman, H. L. Stormer and P. Kim, Nature **462**, 196 (2009).

[69] J. Falson, D. Maryenko, Y. Kozuka, A. Tsukazaki, and M. Kawasaki, Appl. Phys. Exp. **4**, 091101 (2011).

[70] L.N. Pfeiffer, K. W. West, H. L Stormer, and K. W. Baldwin, Appl. Phys. Lett. **55**, 1888 (1989).

[71] M.J. Manfra, Annu. Rev. Condens. Matter Phys. **5**, 347 (2014).

[72] D.G. Schlom and L.N. Pfeiffer, Nature Materials **9**, 881 (2010).

[73] P. L. Kapitza, J. Phys. U.S.S.R **4**, 181 (1941).

[74] N. H. Balshaw, *Practical Cryogenics*, Oxford Instruments Superconductivity Limited, (2001).

[75] M.P. Lilly, K.B. Cooper, J.P. Eisenstein, L.N. Pfeiffer, and K.W. West, Phys. Rev. Lett. **82**, 394 (1999).

[76] R.R. Du, D.C. Tsui, H.L. Stormer, L.N. Pfeiffer, K.W. Baldwin, and K.W. West, Solid State Commun. **109**, 389 (1999).

[77] W. Pan, J.-S. Xia, V. Shvarts, D.E. Adams, H.L. Stormer, D.C. Tsui, L.N. Pfeiffer, K.W. Baldwin, and K.W. West, Phys. Rev. Lett. **83**, 3530 (1999).

[78] J.P. Eisenstein, K.B. Cooper, L.N. Pfeiffer and K.W. West, Phys. Rev. Lett. **88**, 076801 (2002).

[79] J.S. Xia, W. Pan, C.L. Vicente, E.D. Adams, N.S. Sullivan, H.L. Stormer, D.C. Tsui, L.N. Pfeiffer, K.W. Baldwin, and K.W.West, Phys. Rev. Lett **93**, 176809 (2004).

[80] A. Kumar, G.A. Csáthy, M.J. Manfra, L.N. Pfeiffer, and K.W. West, Phys. Rev. Lett. **105**, 246808 (2010).

[81] E. Kleinbaum, A. Kumar, L.N. Pfeiffer, K.W. West, and G.A. Csáthy, Phys. Rev. Lett. **114**, 076801 (2015).

[82] A.A. Zibrov, C. Kometter, H. Zhou, E.M. Spanton, T. Taniguchi, K. Watanabe, M.P. Zaletel, and A.F. Young, Nature **549** 360, (2017).

[83] J.I.A. Li, C. Tan, S. Chen, Y. Zeng, T. Taniguchi, K. Watanabe, J. Hone, and C.R. Dean, Science **358**, 648 (2017).

[84] J. Falson, D. Maryenko, B. Friess, D. Zhang, Y. Kozuka, A. Tsukazaki, J.H. Smet, and M. Kawasaki, Nature Physics **11**, 347 (2015).

[85] M.P. Zaletel, R.S.K. Mong, F. Pollmann, and E.H. Rezayi, Phys. Rev. B **91**, 045115 (2015).

[86] N. Read and E. Rezayi, Phys. Rev. B **59**, 8084 (1999).

[87] E.H. Rezayi and N. Read, Phys. Rev. B **79**, 075306 (2009).

[88] N. Deng, A. Kumar, M.J. Manfra, L.N. Pfeiffer, K.W. West, and G.A. Csáthy, Phys. Rev. Lett. **108**, 086803 (2012).

[89] N. Samkharadze, K.A. Schreiber, G.C. Gardner, M.J. Manfra, E. Fradkin, and G.A. Csáthy, Nature Phys. **12**, 191 (2016).

[90] K.A. Schreiber, N. Samkharadze, G.C. Gardner, R.R. Biswas, M.J. Manfra, and G.A. Csáthy Phys. Rev. B **96**, 041107 (2017).

[91] N. Deng, J.D. Watson, L.P. Rokhinson, M.J. Manfra, and G.A. Csáthy, Phys. Rev. B **86**, 201301 (2012).

[92] C. Zhang, C. Huan, J.S. Xia, N.S. Sullivan, W. Pan, K.W. Baldwin, K.W. West, L.N. Pfeiffer, and D.C. Tsui, Phys. Rev. B **85**, 241302 (2012).

[93] J.D. Watson, G.A. Csáthy, and M.J. Manfra, Phys.Rev. Appl. **3**, 064004 (2015).

[94] Q. Qian, J. Nakamura, S. Fallahi, G.C. Gardner, and M.J. Manfra, Nature Commun. **8**, 1536 (2017).

[95] H.C. Choi, W. Kang, S. Das Sarma, L.N. Pfeiffer, and K.W. West, Phys. Rev. B **77**, 081301 (2008).

[96] W. Pan, J.S. Xia, H.L. Stormer, D.C. Tsui, C. Vicente, E.D. Adams, N.S. Sullivan, L.N. Pfeiffer, K.W. Baldwin, and K.W.West, Phys. Rev. B **77**, 075307 (2008).

[97] N. Samkharadze, J.D. Watson, G. Gardner, M.J. Manfra, L.N. Pfeiffer, K.W. West, and G.A. Csáthy, Phys. Rev. B **84**, 121305 (2011).

[98] C.R. Dean, B.A. Piot, P. Hayden, S. Das Sarma, G. Gervais, L.N. Pfeiffer, and K.W. West, Phys. Rev. Lett. **100**, 146803 (2008).

[99] C. Reichl, J. Chen, S. Baer, C. Rössler, T. Ihn, K. Ensslin, W. Dietsche, and W. Wegscheider, New Journal of Physics **16**, 023014 (2014).

[100] V.J. Goldman, M. Shayegan, and D. C. Tsui, Phys. Rev. Lett. **61**, 881 (1988).

[101] W. Pan, H.L. Stormer, D.C. Tsui, L.N. Pfeiffer, K.W. Baldwin, and K.W. West, Phys. Rev. Lett. **88**, 176802 (2002).

[102] G. Gervais, L.W. Engel, H.L. Stormer, D.C. Tsui, K.W. Baldwin, K.W. West, and L.N. Pfeiffer, Phys. Rev. Lett. **93** 266804 (2004).

[103] C.R. Dean, private communication

[104] N. Deng, G.C. Gardner, S. Mondal, E. Kleinbaum, M.J. Manfra, and G.A. Csáthy, Phys. Rev. Lett. **112**, 116804 (2014).

[105] N. Samkharadze, A. Kumar, M.J. Manfra, L.N. Pfeiffer, K.W. West and G.A. Csáthy, Rev. Sci. Instrum. **82** 053902 (2011).

[106] W. Zhu, S.S. Gong, F.D.M. Haldane, and D.N. Sheng, Phys. Rev. Lett. **115**, 126805 (2015).

[107] R.S.K. Mong, M.P. Zaletel, F. Pollmann, and Z. Papić, Phys. Rev. B **95**, 115136 (2017).

[108] K. Pakrouski, M. Troyer, Y.-L. Wu, S. Das Sarma, M.R. Peterson, Phys. Rev. B **94**, 075108 (2016).

[109] J. Shabani, Y. Liu, and M. Shayegan, Phys. Rev. Lett. **105**, 246805 (2010).

[110] Y. Liu, D. Kamburov, M. Shayegan, L.N. Pfeiffer, K.W. West, and K.W. Baldwin, Phys. Rev. Lett. **107**, 176805 (2011).

[111] W.E. Chickering, J.P. Eisenstein, L.N. Pfeiffer, and K.W. West, Phys. Rev. B **87**, 075302 (2013).

[112] J. Nuebler, V. Umansky, R. Morf, M. Heiblum, K. von Klitzing, and J. Smet, Phys. Rev. B **81**, 035316 (2010).

[113] S.M. Girvin, Phys. Rev. B **29**, 6012 (1984).

[114] V. Shingla, E. Kleinbaum, A. Kumar, L.N. Pfeiffer, K.W. West, and G.A. Csáthy, Phys. Rev. B **108**, 086803 (2018).

[115] Y.P. Chen, R.M. Lewis, L.W. Engel, D.C. Tsui, P.D. Ye, L.N. Pfeiffer, and K.W. West, Phys. Rev. Lett. **91**, 016801 (2003).

[116] R.M. Lewis, Y.P. Chen, L.W. Engel, D.C. Tsui, P.D. Ye, L.N. Pfeiffer, and K.W. West, Physica E **22**, 104 (2003).

[117] P.D. Ye, L.W. Engel, D.C. Tsui, R.M. Lewis, L.N. Pfeiffer, and K.W. West, Phys. Rev. Lett. **89**, 176802 (2002).

[118] R.L. Willett and L.N. Pfeiffer, Surf. Sci. **361**, 38 (1996).

[119] D.R. Leadley, R.J. Nicholas, C.T. Foxon, and J.J. Harris, Phys. Rev. Lett. **72**, 1906 (1993).

[120] A.S Yeh, H.L. Stormer, D.C. Tsui, L.N. Pfeiffer, K.W. Baldwin, and K.W. West, Phys. Rev. Lett. **82**, 592 (1999).

[121] W.Pan, H.L. Stormer, D.C. Tsui, L.N. Pfeiffer, K.W. Baldwin, and K.W. West, Phys. Rev. B, **61**, R5101 (2000).

[122] W.Pan, H.L. Stormer, D.C. Tsui, L.N. Pfeiffer, K.W. Baldwin, and K.W. West, Phys. Rev. Lett. **88**, 176802 (2002).

[123] X. Zu, K. Park, and J.K. Jain, Phys. Rev. B **61**, R7850 (2000).

[124] K. Park and J.K. Jain, Solid State Comm. **119**, 291 (2001).

[125] A.C. Balram, Csaba Töke, A. Wójs, and J.K Jain, Phys. Rev. B. **91**, 045109 (2015).

[126] A.C. Balram, Phys. Rev. B. **94**, 165303 (2016).

[127] W. Li, D.R. Luhman, D.C. Tsui, L.N. Pfeiffer, and K.W. West, Phys. Rev. Lett. **105**, 076803 (2010).

[128] Y. Liu, C.G. Pappas, M. Shayegan, L.N. Pfeiffer, K.W. West, and K.W. Baldwin, Phys. Rev. Lett. **109**, 036801 (2012).

[129] Y. Liu, D. Kamburov, S. Hasdemir, M. Shayegan, L.N. Pfeiffer, K.W. West, and K.W. Baldwin, Phys. Rev. Lett. **113**, 246803 (2014).

[130] A. Hatke, Y. Liu, B.A. Magill, B.H. Moon, L.W. Engel, M. Shayegan, L.N. Pfeiffer, K.W. West, and K.W. Baldwin, Nat. Comm. **5**, 4154 (2014).

[131] Y. Liu, D. Kamburov, M. Shayegan, L. N. Pfeiffer, K. W. West, and K. W. Baldwin, Phys. Rev. Lett. **107**, 176805 (2011).

[132] C. Zhang, C. Huan, J.S. Xia, N.S. Sullivan, W. Pan, and K.W. Baldwin, Phys. Rev. B **85**, 241302(R) (2012).

[133] C. Zhang, C. Huan, J.S. Xia, N.S. Sullivan, W. Pan, K.W. Baldwin, K.W. West, L.N. Pfeiffer, and D.C. Tsui, Phys. Rev. B **85**, 241302 (2012).

[134] S. Chen, R. Ribeiro-Palau, K. Yang, K. Watanabe, T. Taniguchi, J. Hone, M. O. Goerbig, and C. R. Dean, Phys. Rev. Lett. **122**, 026802 (2019).

[135] D. Maryenko, A. McCollam, J. Falson, Y. Kozuka, J. Bruin, U. Zeitler, and M. Kawasaki, Nat. Commun. **9**, 4356 (2018).

[136] N. Shibata and D. Yoshioka, J. Phys. Soc. Jpn. **72**, 664 (2003).

[137] M. O. Goerbig, P. Lederer, and C.M. Smith, Phys. Rev. B **68**, 241302 (2003)

[138] H.W. Jiang, R.L. Willett, H.L. Stormer, D.C. Tsui, L.N. Pfeiffer, and K.W. West, Phys. Rev. Lett. **65**, 633 (1990).

[139] N. Samkharadze, D. Ro, L. N. Pfeiffer, K. W. West, and G. A. Csáthy, Phys. Rev. B **96**, 085105 (2017).

[140] D. Ro, N. Deng, J. D. Watson, M. J. Manfra, L. N. Pfeiffer, K. W. West, and G. A. Csáthy, Phys. Rev. B **99**, 201111(R) (2019).

[141] H. Zhu, Y.P. Chen, P. Jiang, L.W. Engel, D.C. Tsui, L.N. Pfeiffer, and K.W. West, Phys. Rev. Lett. **105**, 126803 (2010).

[142] Y. Liu, D. Kamburov, S. Hasdemir, M. Shayegan, L.N. Pfeiffer, K.W. West, and K.W. Baldwin, Phys. Rev. Lett. **113**, 246803 (2014).

[143] A. Hatke, Y. Liu, B.A. Magill, B.H. Moon, L.W. Engel, M. Shayegan, L.N. Pfeiffer, K.W. West, and K.W. Baldwin, Nat. Comm. **5**, 4154 (2014).

[144] H. Yi and H.A. Fertig, Phys. Rev. B **58**, 4019 (1998).

[145] S.Y. Lee, V.W. Scarola, and J.K. Jain, Phys. Rev. B **66**, 085336 (2002).

[146] M.O. Goerbig, P. Lederer, and C.M. Smith, Phys. Rev. Lett. **93**, 216802 (2004).

[147] C.C. Chang. G.S. Jeon, and J.K. Jain, Phys. Rev. Lett. **94**, 016809 (2005).

[148] A.C Archer, and J.K. Jain, Phys. Rev. B **84**, 115139 (2011).

[149] A.C Archer, K. Park, and J.K. Jain, Phys. Rev. Lett. **111**, 146804 (2013).

PUBLICATIONS

1. Finite-temperature behavior in the 2nd Landau level of the two-dimensional electron gas
   V. Shingla, E. Kleinbaum, A. Kumar, L.N. Pfeiffer, K.W. West and G. Csathy, Phys. Rev. B 97, 241105 (2018)

2. Stabilizing a SQUID based current amplifier in high magnetic fields
   V. Shingla, E. Kleinbaum, A. Kumar, L.N. Pfeiffer, K.W. West and G. Csathy, Meas. Sci. and Tech. **29**, 10 (2018)

3. SQUID-based current sensing noise thermometry for quantum resistors at dilution refrigerator temperatures
   E. Kleinbaum, **V. Shingla**, G. Csathy, Rev. Sci. Inst. **88**, 034902 (2017)

4. Observation of a novel crystal of quasiholes in the lowest Landau level
   V.Shingla, L.N. Pfeiffer, K.W. West and G. Csathy, *manuscript in preparation*

5. Reentrant Fractional Quantum Hall state : a novel solid of composite fermions
   V.Shingla, A. Kumar, L.N. Pfeiffer, K.W. West and G. Csathyl, *manuscript in preparation*